


2019

## Lithium Polysulfide Battery with Improved Capacity and Cycle Performance using Carbon Black Coated Free-standing Carbon Cloth

Zhen Wei  
*University of Central Florida*

 Part of the [Engineering Science and Materials Commons](#)  
Find similar works at: <https://stars.library.ucf.edu/etd>  
University of Central Florida Libraries <http://library.ucf.edu>

This Masters Thesis (Open Access) is brought to you for free and open access by STARS. It has been accepted for inclusion in Electronic Theses and Dissertations by an authorized administrator of STARS. For more information, please contact [STARS@ucf.edu](mailto:STARS@ucf.edu).

---

### STARS Citation

Wei, Zhen, "Lithium Polysulfide Battery with Improved Capacity and Cycle Performance using Carbon Black Coated Free-standing Carbon Cloth" (2019). *Electronic Theses and Dissertations*. 6784.  
<https://stars.library.ucf.edu/etd/6784>

LITHIUM POLYSULFIDE BATTERY  
WITH IMPROVED CAPACITY AND CYCLE PERFORMANCE  
USING CARBON BLACK COATED FREE-STANDING CARBON CLOTH

by

ZHEN WEI

B.S. Zhengzhou University, Materials Science and Engineering, Zhengzhou, 2016

A thesis submitted in partial fulfillment of the requirements  
for the degree of Master of Science  
in the Department of Materials Science Engineering  
in the College of Engineering and Computer Sciences  
at the University of Central Florida  
Orlando, Florida

Fall Term  
2019

Major Professor: Akihiro Kushima

© 2019 Zhen Wei

## ABSTRACT

Lithium ion batteries (LIBs) have been used in various applications such as portable electronics, grid storages, and electric vehicles (EVs). Despite its commercial success, further advancement of the battery is necessary to satisfy the increasing demands for low-cost and high- performance energy storage devices as LIB is reaching its theoretical limits. Lithium sulfur battery (LSB) is one of the promising candidates for the next generation energy storage technologies. LSB uses sulfur cathode which is a low-cost and earth abundant material with an extremely high theoretical capacity of 2600 Wh kg<sup>-1</sup>. Although there have been numerous researches aiming to establish the LSB technology, it is still in a development stage. Some of the major challenges are; low-electric conductivity, dissolution of the intermediate lithium-polysulfide reactants, and the low Coulombic efficiency. These issues must be overcome before LSBs can become practical.

The objective of this work is to develop an LSB cathode that solves the above issues and contributes to advancing the development of the LSB technology. We focus on improving the electrical conductivity while reducing the shuttle effect, a parasitic reaction of the polysulfides at the anode lithium surface. To achieve this goal, we developed a carbon black coated free-standing carbon cloth. It is infiltrated with a Li<sub>2</sub>S<sub>8</sub>-containing catholyte as an active material, and its carbon framework serves as an entrapment of the polysulfides. The electrode composite enabled high- sulfur-loading, and its high surface area increased the reaction sites allowing the effective utilization of the sulfur that lead to the high capacity. It also showed high capacity retention by successfully trapping the polysulfides within the electrode. This facile and low-cost solution contributes to the realization of the LSBs.

Dedicated to my parents

## **ACKNOWLEDGMENTS**

This work was implemented in Professor Akihiro Kushima's group at the University of Central Florida (UCF). Here, it is with my pleasure that I acknowledge every single individual who has accompanied with me and contributed to my work in the past.

I would like to first and foremost express my deep appreciation and gratitude to my advisor, Professor Akihiro Kushima, for his unconditional guidance, support and inspiration all the way from when I just joined his research group through the completion of my degree. This thesis would not have been possible without his inspiration, ideas and support. I would also like to thank all my committee members, Professor Yang Yang and Xiaofeng Feng for their time and the valuable feedback and thought-provoking suggestions.

It has been a great pleasure to work with my current colleagues in Dr.Kushima's research group, who have helped me and inspired me in many ways: Saisaban Fahad, Supriya Koul and Megan Aubin. I am deeply indebted to Saisaban Fahad, who offered invaluable research inspirations and guidance. I also would like to appreciate Mr. Krik Scammon and Materials Characterization Facility (MCF) for assistance on material characterization.

Most of all, I would not be here where I am now without my parents — my best friends, my soulmates in this world — who know how to cheer me up when I felt lost.

## TABLE OF CONTENTS

LIST OF FIGURES .....	viii
LIST OF TABLES .....	xiii
CHAPTER 1 INTRODUCTION.....	1
1.1 Background and Motivation .....	1
1.2 Objective of the research .....	6
CHAPTER 2 LITERATURE REVIEW .....	7
2.1 Principle of rechargeable lithium sulfur battery system .....	7
2.2 Technical issues and challenges for LSB .....	14
2.2.1 Lithium metal anode (negative electrode) .....	15
2.2.2 Electrolyte .....	17
2.2.3 Sulfur-based cathode (positive electrode).....	19
2.3 Approaches to overcome the serious issues and challenges .....	23
2.3.1 Modification of sulfur-based cathode .....	23
2.3.1.1 Synthesis of sulfur-carbon composite .....	23
2.3.2 Application of an interwoven self-supporting carbon nanotube layer .....	49
CHAPTER 3 POLYSULFIDE INFILTRATED FREE-STANDING CARBON CLOTH WITH CARBON BLACK COATING.....	51

3.1 Overview .....	51
3.2 Materials preparation .....	51
3.2.1 Preparation of carbon-black-coated carbon cloth .....	51
3.2.2 Preparation of electrolyte .....	53
3.2.3 Coin cell assembly .....	53
3.3 Sample morphology before cycling.....	54
3.4 Electrochemical characterization.....	58
3.4.1 Cyclic voltammetry (CV) .....	58
3.4.2 Galvanostatic charge-discharge cycling .....	59
3.4.3 Characterization of the samples after cycling .....	61
CHAPTER 4     CONCLUSION .....	64
REFERENCES.....	65



## LIST OF FIGURES

Figure 1- 1 Comparison of literature growth from 1987 to 2017 in the field of search[6].	2
Figure 1- 2 (A) The gravimetric capacities of several metal anodes (B) The volumetric capacities of several metal anodes (C) The gravimetric and volumetric energy densities of those metal anodes when coupled with an 4V cathode [4].	2
Figure 1- 3 The increasing sales of lithium ion battery over the past two decades [10].	3
Figure 1- 4 Comparison of theoretical specific energy density, capacity and voltage plateau of different cathode materials [1].	4
Figure 1- 5 Schematic representation of shuttle effect in a typical LSB [3].	6
Figure 2- 1 Schematic representation of working mechanism of a representative lithium sulfur battery [18].	7
Figure 2- 2 The functions of polymeric binders involved in LSB [31].	10
Figure 2- 3 Schematic illustration of cycling curves of charging and discharging exhibiting the oxidation and the reduction [8].	12
Figure 2- 4 The typical issues that lithium metal anode face [37].	15
Figure 2- 5 Lithium dendrite formation in a lithium battery [39].	16
Figure 2- 6 Schematic diagram of components of a typical lithium sulfur battery with electrolyte consisting of lithium salts [42].	17
Figure 2- 7 A schematic illustration of the working principles of (a) graphite/LiCoO <sub>2</sub> lithium-ion battery and (b) lithium–sulfur battery [45].	20
Figure 2- 8 Schematic diagram of self-discharging at different periods [18].	22
Figure 2- 9 Schematic diagram of TEM image of carbon sphere (a,b) and sulfur-carbon composite (c)	

high-angle annular dark field-scanning TEM image (d) EDX spectrum (e) corresponding line scans [52].	25
Figure 2- 10 Schematic diagram of electrochemical performance of S/(CNT@MPC) composite and comparison with traditional S/CB composite [53].	26
Figure 2- 11 SEM images of CMK-3/S and its electrochemical performance. a, CMK-3/S before thermal treatment. b, thermally treated CMK-3/S at 155 oC, demonstrating that elemental sulfur disappears. c,d, comparison of galvanostatic charge-discharge curves between CMK-3/S with heating and CMK-3/S without heating [54].	27
Figure 2- 12 a, CMK-3/S heated at 155oC b, magnified image c,d, uniform distribution of sulfur and carbon e, schematic diagram of elemental sulfur constrained in the highly ordered interconnected pores of CMK-3 f, schematic diagram of the process of composite synthesis [54].	28
Figure 2- 13 Schematic diagram of fabrication of hollow carbon nanofiber/sulfur composite through melt infusion. (a) the high aspect ratio of hollow carbon nanofiber array (b) fabrication process of hollow carbon nanofiber array/sulfur composite (c) before and after carbon coating and sulfur infusion [55].	29
Figure 2- 14 (a) TEM image of DHCS (b) FESEM image of DHCS-S composite (c) and (d) TEM images of DHCS-S composite (e) EDX showing the elemental distribution [56].	31
Figure 2- 15 (a) TEM image of carbon matrix (b) magnified TEM image of graphitic structure (c) schematic illustration of melt adsorption-solvent extraction [57].	32
Figure 2- 16 (a) TEM image of mesoporous carbon hollow spheres (b) prepared carbon/sulfur composite (c) schematic illustration of EDX showing the distribution of sulfur [58].	33
Figure 2- 17 schematic illustration of synthesis of sulfur-impregnated disordered carbon nanotubes [59].	34
Figure 2- 18 SEM and TEM images of disordered carbon nanotubes through the approach of wetting technique [59].	35
Figure 2- 19 (a) schematic diagram of assembly of membrane by the evaporation technique (b) S- CNT membrane (c) SEM image of S-CNT network structure (d) stress-strain curve of S-CNT (e) electrical stability of membrane [60].	36

Figure 2- 20 (a) Raman spectra of CNTs, sulfur and S-CNT-23 (b) HRTEM image of microstructure of S-CNT-23 (c) STEM image of S-CNT-23 and elemental distribution [60].	37
Figure 2- 21 (a) Fast capacity decay and low Coulombic efficiency can be induced by the parasitic dissolution of polysulfide species and volume expansion during lithiation process when bare sulfur particles are used in LSB system. (b) Even if the core-shell morphological structure offers a coating layer performing the protective duty. However, the cracks will still form on the surface of the shell when the core-shell goes through volume expansion during lithiation and the subsequent polysulfide dissolution will occur as well. (c) The yolk-shell morphological structure is much more advantageous than the conventional core-shell structure due to enormously large inner space, which can effectively accommodate the volume expansion during the lithiation process and can successfully maintain the structural integrity to realize effective entrapment of soluble polysulfide species [61].	39
Figure 2- 22 (a) Schematic illustration of synthesis that consists of the formation of core-shell morphological structure done by coating the bare sulfur particles with TiO <sub>2</sub> and the subsequent formation of the yolk-shell structure achieved by dissolution of sulfur in toluene (b) SEM images of fabricated yolk-shell morphological structure (c) TEM images of synthesized yolk-shell structure [61].	39
Figure 2- 23 Schematic diagram of heterogeneous sulfur crystal growth mechanism [62].	40
Figure 2- 24 (a) and (b) FESEM images of sulfur-impregnated graphene composite (c) and (d) bright filed TEM image and dark field TEM image of sulfur-impregnated graphene composite [62].	41
Figure 2- 25 Schematic diagram of fabrication of sulfur-MWCNT composite cathode [63].	42
Figure 2- 26 (a) SEM image of interwoven MWCNTs (b) morphology of S-CNT-A sample (c) elemental mapping [63].	42
Figure 2- 27 Schematic illustration of synthesis of graphene-sulfur composite [64].	44
Figure 2- 28 SEM images of graphene-sulfur composite (a) at low magnification and (b) at high magnification [64].	44
Figure 2- 29 Schematic illustration of one pot synthesis of graphene-sulfur composite [65].	45
Figure 2- 30 Schematic of diagram of synthesis steps of cathode preparation [66].	47

Figure 2- 31 SEM images of (a) CNTs (b) sulfur/VA-CNT composite (c) as-cycled sulfur/VA- CNT composite [66].	47
Figure 2- 32 Schematic diagram of synthesis steps of sulfur-CNTs [67].	48
Figure 2- 33 Characterization of CNTs (a) before H <sub>2</sub> O <sub>2</sub> treatment and (b) after H <sub>2</sub> O <sub>2</sub> treatment (c) SCNT before heat treatment (d) SCNT after heat treatment (e)and (f) TEM image of SCNT after heat treatment [67].	49
Figure 2- 34 Schematic diagram of the configuration of lithium sulfur battery (a) conventional configuration without the interlayer (b) novel configuration with WMCNT paper [68].	50
Figure 2- 35 Schematic diagram of morphology of MWCNT paper (a) before charge-discharge process (b) after 100 cycles (c) the morphology of raw tube before charge-discharge process (d) the structure of swollen tube after cycling (e) elemental mapping [68].	50
Figure 3- 1 Optical micrograph of carbon-black-coated carbon cloth	52
Figure 3- 2 Schematic diagram of Li <sub>2</sub> S <sub>8</sub> -containing catholyte.	52
Figure 3- 3 Schematic diagram of coin cell assembly	53
Figure 3- 4 (a-b) SEM images of interwoven self-supporting carbon cloth without carbon black coating. (c-d) SEM images of self-weaving carbon cloth with carbon black coating.	55
Figure 3- 5 Microstructural characterization of dissolved polysulfide electrode. (a-c) SEM images of sulfur-infiltrated carbon cloth without coating before cycling. (d-f) SEM images of sulfur-infiltrated carbon cloth with coating before cycling.	56
Figure 3- 6 (a-c) EDS data of sulfur-infiltrated carbon cloth without coating before cycling. (d-f) EDS data of sulfur-infiltrated carbon cloth with coating before cycling.	57
Figure 3- 7 Cyclic voltammograms of the Li/dissolved polysulfide batteries with uncoated carbon cloth and coated carbon cloth at a scan rate of 0.1 mV s <sup>-1</sup> .	59
Figure 3- 8 a) Voltage vs discharge capacity and charge capacity profiles of the 1st at 0.1C, 1 <sup>st</sup> , 50th, 100th at 0.2 C for uncoated carbon cloth. (b) Cyclability and Coulombic efficiency of the cell with uncoated carbon cloth. (c) Voltage vs discharge capacity and charge capacity profiles of the 1st at 0.1C,	

1st ,50th , 100th at 0.2 C for coated carbon cloth. (d) Cyclability and Coulombic efficiency of the cell with coated carbon cloth. ....59

Figure 3- 9 (a-c) SEM images of Li<sub>2</sub>S<sub>8</sub>-infiltrated carbon cloth without coating after cycling. (d-f) SEM images of Li<sub>2</sub>S<sub>8</sub>-infiltrated carbon cloth with coating after cycling. ....61

Figure 3- 10 (a-b) SEM images of cycled anode of uncoated sample after cycling. (c-d) SEM images of cycled anode of coated sample after cycling .....62

## **LIST OF TABLES**

Table 1- 1 Specifications of a prototype lithium-sulfur battery fabricated by OXIS energy [15]. .....	5
---	---

# CHAPTER 1 INTRODUCTION

## 1.1 Background and Motivation

To deal with environmental and social issues such as global warming, limited fossil fuel supplies, and pollutions, development of renewable energy technologies are attracting continuous attentions [1]. Researchers have been giving much efforts to developing novel, clean, environmentally benign and sustainable energy choices to mitigate these issues. Wind and solar energy can be converted to electricity with cleaner techniques and higher efficiencies [2], and photovoltaic panels and flywheels are being installed worldwide. However, their unstable nature as an energy source limits their applications [3]. As one of the most important advanced technologies in the contemporary history [4], lithium ion batteries (LIBs) have tremendously reshaped people's lifestyles and received more and more attention from scientific community since the very first commercialization was achieved by Sony in the early 1990s [5]. Figure 1-1 shows that there was a significant increase in research works related to batteries over the past from 2010 to 2017, a considerable amount of papers regarding the rapid development of battery technology have been published by researchers all over the world [6]. It is strongly believed that continuous dedication to batteries leads to continuous enhancements of batteries' derivative descendants that might determine the future of energy and our lifestyle [7]. LIB has been frequently used in portable electronic devices, small appliances and some electric vehicles due to its exceptional performance [8]. The desired incorporation of small atomic weight, considerably low reduction potential, and monovalent charge provides lithium with overwhelming advantages over other energy storage technologies [9].

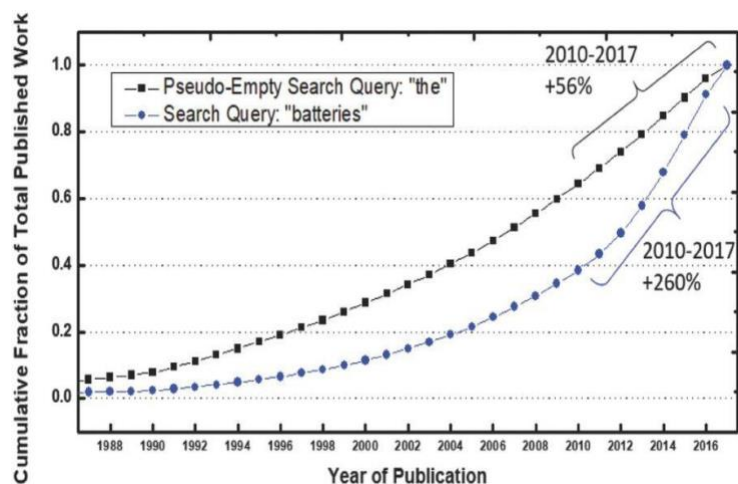


Figure 1- 1 Comparison of literature growth from 1987 to 2017 in the field of search[6].

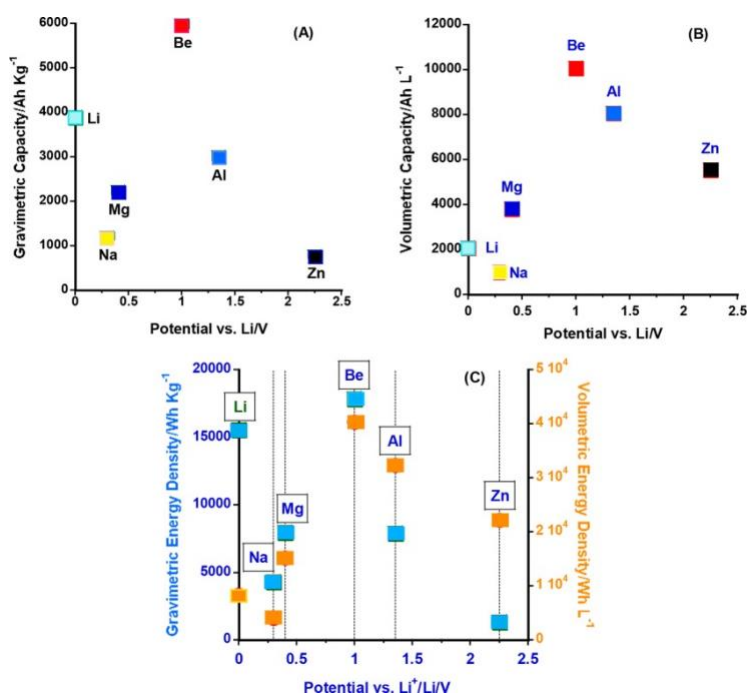


Figure 1- 2 (A) The gravimetric capacities of several metal anodes (B) The volumetric capacities of several metal anodes (C) The gravimetric and volumetric energy densities of those metal anodes when coupled with an 4V cathode [4].

Lithium has a significantly high gravimetric capacity of  $3860 \text{ mAh g}^{-1}$  and the lowest standard reduction potential of  $-3.04 \text{ V}$ . Figure 1-2 shows that lithium has the second highest gravimetric capacity



among all the discovered elements and is only lower than Be (5950 mAh g<sup>-1</sup>). However, there are several elements with higher volumetric capacities than that of Li owing to their multivalent characters. However, the multivalence property can leads to some issues. The cations of those elements (Be<sup>2+</sup>, Al<sup>3+</sup>, Zn<sup>2+</sup>, and Mg<sup>2+</sup>) that have the similar size as Li<sup>+</sup> carrying double or triple charges create huge obstacles that prevent themselves from freely diffusing in an environment around them [4]. In fact, LIB has been expanding its share as shown in Figure 1-3. Current LIB delivers gravimetric energy density of approximately 100-150 Wh/kg, which is much improved from the initial commercialization released by Sony.

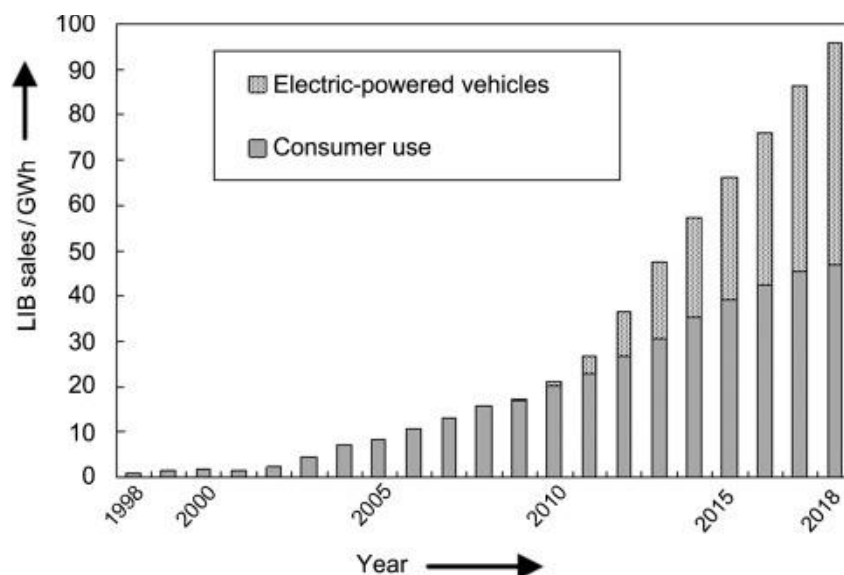


Figure 1- 3 The increasing sales of lithium ion battery over the past two decades [10].

Although advanced technology of lithium ion battery has conquered the portable electronic devices markets and is still being improved, its limited energy density falls short of meeting the requirements determined by the powering of both hybrid electric vehicles and electric vehicles [11]. Possibilities of drastic enhancement of lithium ion battery's energy density seems to be very slim for researchers and scientists since lithium ion battery has apparently reaching its theoretical limit. Therefore,

there is an urgent need for developing the next-generation high-performance energy storage systems with considerably high energy density that can meet the requirements of the highly demanding applications. In the past few years, the focus of scientists' attention has shifted to sulfur, one of the most earth abundant elements. It is one of the promising candidates for the cathode material due to its exceptional theoretical specific capacity of approximately 1675 mAh/g and considerably high energy density of approximately 2500 Wh/kg [12-13]. Sulfur exhibits one of the highest theoretical specific capacities among all existing positive electrode materials, which is an order of magnitude higher than those of transition-metal oxide cathodes [14]. The coupling of the two high-capacity electrodes, lithium sulfur battery (LSB), renders an average cell voltage of 2.2V and a theoretical specific energy of 2570 Wh/kg as schematically shown in Figure 1-4.

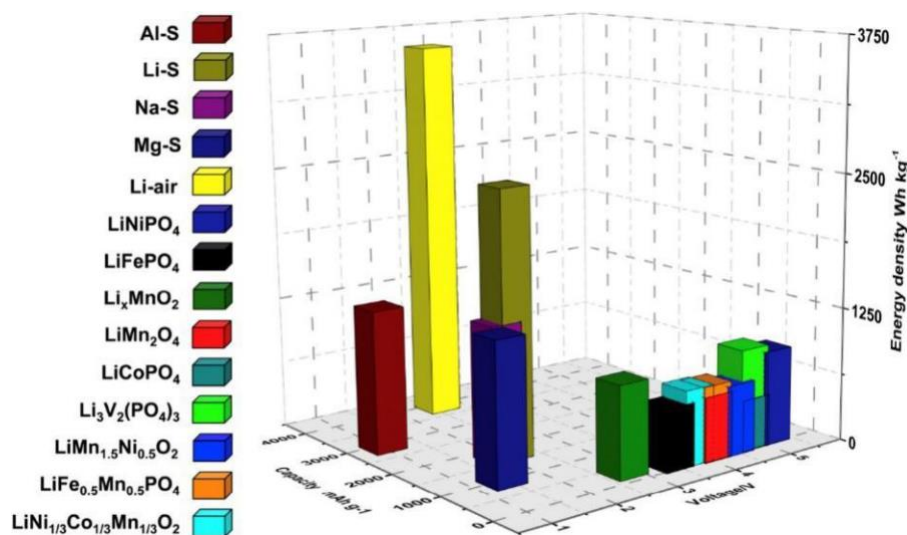


Figure 1- 4 Comparison of theoretical specific energy density, capacity and voltage plateau of different cathode materials [1].

Table 1- 1 Specifications of a prototype lithium-sulfur battery fabricated by OXIS energy [15].

Type	Rechargeable Lithium-Sulfur Pouch Cell Remarks: Li Metal Anode
cell dimension	176 mm × 114 mm × 13.7 mm
maximum voltage	2.45 V
nominal voltage	2.05 V
capacity	21 Ah (at 0.2 C, 30 °C)
weight	233 ± 5 g
volume	0.252 L
recommended charging condition in applications	2.1 A constant current (C/10) at 30 °C (charge stop at 2.45 V or 11 h max charge time)
recommended discharging condition in applications	peak discharge current: 2 C maximum continuous discharge current (at 30 °C): 1.5 C
maximum continuous power	60 W (at 30 °C)
optimum operating temperature	30 °C
Cycle number before getting 80% of the beginning-of-life capacity	180 cycles (cycled at 30 °C in a standard life test regime)

Its merits of high natural abundance, an inherently low competitive cost, non-toxicity and easy purification techniques make it highly appealing to the scientific community. For example, a prototype battery fabricated by OXIS Energy Ltd exhibits the energy density of 600 Wh/kg. The specifications of the cell are shown in Table 1-1 [15]. However, there are various challenges and drawbacks of sulfur that requires to be circumvented to make it suitable when coupled with the lithium metal anode [16]. For example, the complex reaction mechanism of sulfur-based cathode with lithium produces a series of intermediate lithium polysulfides. These sulfur intermediates can easily dissolve in the electrolyte, reach the lithium anode, and lead to parasitic reactions (shuttle effect) as schematically illustrated in Figure 1-5. Once soluble polysulfides travel through the electrolyte and reach the anode, it forms insoluble  $\text{Li}_2\text{S}_2/\text{Li}_2\text{S}$  with insulating nature passivating the electronically conducting surface of the anode. It also causes the loss of active material, low Coulombic efficiency and formidable self-discharge behavior with the continuous cycling process [16]. Additionally, insulating nature of Sulfur and its large

volume changes during charge/discharge process causes a low cycle life time of LSB [17-21].

## 1.2 Objective of the research

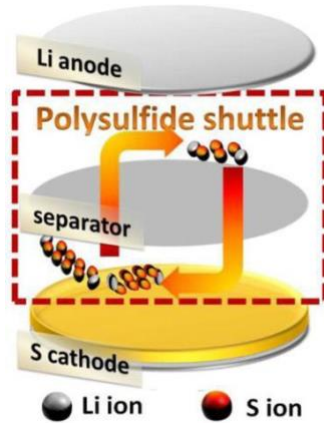


Figure 1- 5 Schematic representation of shuttle effect in a typical LSB [3].

Preventing the dissolution and diffusion of the lithium polysulfide species is a key to the success of LSB technology. The main objective of this work is to enhance the electrochemical performance of the rechargeable LSB system primarily focusing on the cathode design. To achieve this goal, a carbon black coated free-standing carbon cloth performing double duties as a current collector and a sulfur trapping host infiltrated with a sulfur-containing liquid-phase lithium polysulfides (catholyte) is developed. This current collector-free and high-sulfur-loading cathode with a facile dispersion and uniform distribution of active material in the highly conducting carbon cloth matrix was accomplished by simple and facile infiltration of lithium polysulfide [22]. Self-supporting carbon cloth-based electrode coated with carbon black of Li/dissolved polysulfide battery with abundant spaces is beneficial for trapping charged/discharged products and electrolyte penetration, leading to unprecedented discharge capacity.

## CHAPTER 2 LITERATURE REVIEW

### 2.1 Principle of rechargeable lithium sulfur battery system

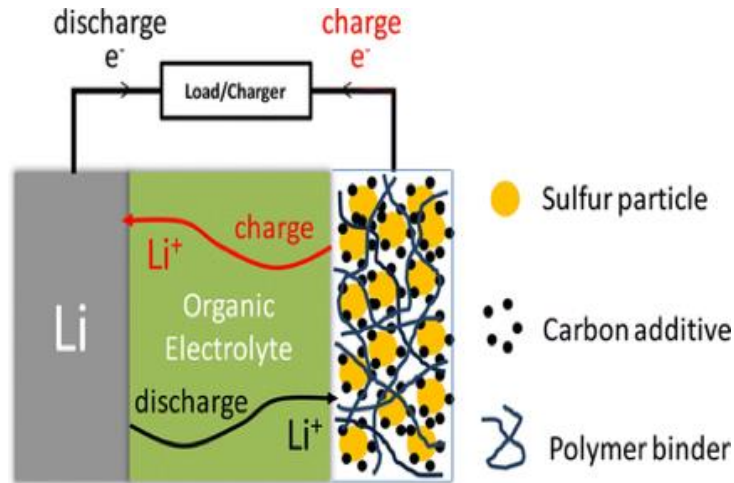


Figure 2- 1 Schematic representation of working mechanism of a representative lithium sulfur battery [18].

Since sulfur-based cathode was proposed for the first time in the early 1960s, enormous amount of attempts have been undertaken to develop the metal-sulfur batteries and LSB [23]. The essential components of a typical lithium sulfur battery are schematically shown in Figure 2-1. It consists of three essential constituents:

**Anode:** In most cases, lithium metal is selected due to its high capacity and the lowest standard reduction potential [24-25].

**Electrolyte:** Organic electrolyte has been widely used because of its compatibility with the other three key components in LSB (the sulfur-based cathode, the lithium metal anode and the produced intermediates of sulfur during charge/discharge process). It is essential to take other major properties (e.g. ionic conductivity, voltage window, viscosity when heated, etc.) into account when choosing ideal

material for electrolyte. Extensive efforts have been made to find an electrolyte with optimum performance.

**Cathode:** Various sulfur-composite materials have been developed to improve the LSB performance.

Additionally, several other components are assembled in a single coin cell apart from the three key components depending on various manufacturing approaches, coin cell designing method and mode of charge-discharge process. These supporting materials are listed below:

**Current collector:** A current collector is typically employed for sulfur-based cathode in the battery system. Sulfur containing slurry is coated on planar current collector to construct the sulfur-based cathode. Aluminum is the most extensively used material for the current collector because of its extraordinarily high electronic conductivity and the low cost. Being able to form a protective oxide layer is an appealing quality that can effectively prevent corrosion to happen during charge-discharge process some other promising alternatives (e.g. carbon cloth, nickel-foam, graphene, carbon paper, etc.) are also used as current collectors [26-29]. However, a few limitations and challenges that the conventional current collectors face impede the realization of enhancement in loading mass of active material. The low loading mass of sulfur can be resolved by the introduction of nanostructured current collectors owing to their promising properties. The nanostructured current collectors with superior structural flexibility and hierarchical pores render the functionalized current collectors with enormous free space to accommodate the volume expansion and maintain the structural and mechanical integrity of the electrodes during the repeated charge-discharge cycling process [30].

**Conductive additives:** It is well acknowledged that conductive additives play a significant role in the performance of the rechargeable lithium sulfur battery system and ought to be considered as essential constituent. Under no circumstances, pure sulfur can be chosen to fabricate the cathode because elemental sulfur is an electrical insulator. In order to efficiently transport ions and electrons in the battery system,

there is an urgent need to add a certain amount of conductive additive. Carbon is the most extensively employed material for the conductive additive due to its considerable abundance, low cost, high electronic and ionic conductivity. There are other favorable alternatives (e.g. graphene, graphene oxide, etc.) that have been used in the rechargeable lithium sulfur battery system.

**Binder:** The binders can be classified depending on their major functions, including mechanical property, electric/ionic conductivity, polysulfide regulation, and other special functionalities (schematically shown in Figure 2-2). There is no denying that binder plays an important role in acting like glue strongly binding conductive additive, current collector and the sulfur together and maintaining the morphological and mechanical integrity of the electrode during the repeated charge-discharge cycling process. Polyvinylidene fluoride (PVDF) is the most widely adopted binder in the field of lithium batteries due to its appealing properties such as high adhesive strength, high thermal stability and wide electrochemical window [31]. However, the pulverization of the electrode lowering the overall performance of battery during the repeated charge-discharge cycling can be caused by some inherent properties of PVDF such as its swelling and dissolution in organic electrolyte and low mechanical ductility, especially for sulfur-based cathode in LSB [31]. Serious shuttle effect lowering the overall performance of battery system can be mitigated by exploiting binders with high affinities and redox activity. Strengthening of electronic and ionic contact between sulfur and conductive additives or electrolyte can be realized with the addition of highly conducting binders.

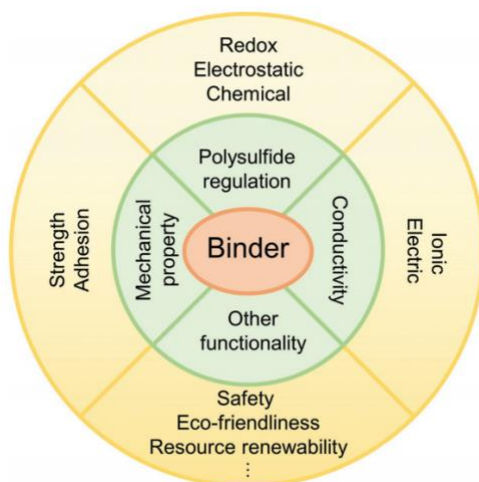


Figure 2- 2 The functions of polymeric binders involved in LSB [31].

**Separator:** Polyethylene (PE), polypropylene (PP), and the mixture of PP/PE separators with numerous tiny pores in the range of micrometers have been extensively utilized and commercialized in the field of lithium batteries. These polyolefin-based separators have received enormous amount of attention owing to its appealing properties, such as high chemical stability, high porosity and low cost. However, the overall performance of batteries is impeded by several limitations and challenges associated with polyolefin separators such as low wettability toward the electrolyte and poor thermal stability. Another drawback is that the cost of large- scale production of highly porous polyolefin separators is very high because of complicated stretching process involved. Stretching along with application of high temperature has a negative impact on the polyolefin separators, because shrinkage of separators can occur.

Re-organization of the stretched polymer chains. The shrinkage poses a real threat to the life span of the battery system. Under normal condition, typical separators are made up of various polymeric materials, glass fibers and other insulating material. Various types of separators are used depending on cell designing mode and electrolyte's chemical properties. For example, a separator made from glass is required to absorb the highly viscous electrolyte and enable electrolyte to make adequate contact



between lithium metal anode and sulfur-based cathode. Polypropylene film (Celgard) is most frequently used separator in the rechargeable lithium sulfur battery system due to exceptional porosity and low density.

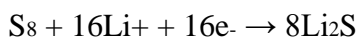
A fundamental understanding of charge-discharge working principle is required to address the challenges and issues that LSB face. In the lithium sulfur battery system, the open-circuit voltage that the battery at open-circuit state gains is directly proportional to the electrochemical potential difference between lithium metal anode and sulfur-based cathode [32]. A manufactured battery is charged in the first place and discharging takes place when the battery is connected to the load. Metallic lithium undergoes the oxidation at the anode (negative electrode) to create lithium ions and electrons. The formed electrons and lithium ions travel through the external circuit and the electrolyte respectively and reach the sulfur- based cathode, and the sulfur on the cathode undergoes a series of reduction reactions by gaining the produced electrons. Opposite conversion can take place in the charging process through reduction of lithium metal anode and oxidation of sulfur-based cathode. The half- cell reaction and the reaction for the whole cell in the discharging process and charging process are listed below [33].

**Lithiation (discharge) process:**

Negative electrode: oxidation reaction (losing electrons)

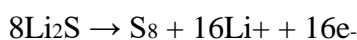


Positive electrode: reduction reaction (gaining electrons)

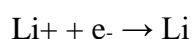


**De-lithiation (charge) process:**

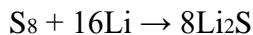
Positive electrode: oxidation reaction (losing electrons)



Negative electrode: reduction reaction (gaining electrons)



The whole electrochemical reaction:



A particularity of the rechargeable LSB system primarily lies in its extremely complex working principle. Although one single step is listed above to describe the whole reaction, the actual reaction consists of multiple steps. The reaction between elemental sulfur and lithium involves a formation of a series of lithium polysulfides as intermediate products. The detailed information of multiple steps that consists of one-phase reduction and two-phase reduction will be shown below and schematically illustrated in Figure 2-3.

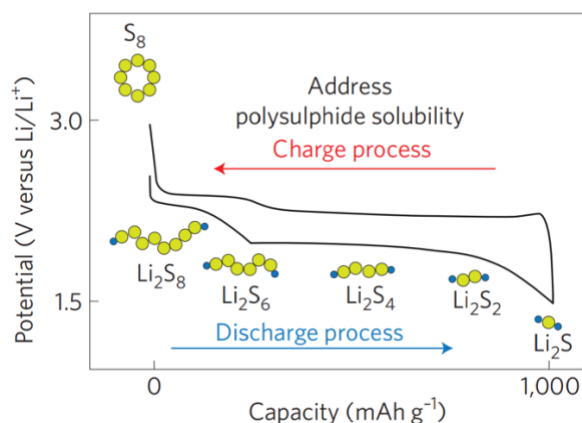
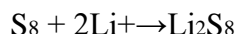


Figure 2- 3 Schematic illustration of cycling curves of charging and discharging exhibiting the oxidation and the reduction [8].

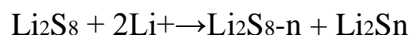
Figure 2-3 shows different products at various stages of redox in the lithium sulfur battery system. The extremely complex mechanism of multi-step reduction in the rechargeable lithium sulfur battery system has been a heated topic for many years in the scientific community. Extensive effort has been made to quest for more convincing statement about the underlying mechanism of multi-step reduction. An informative research review regarding reduction mechanism published by Wild et al. is shown below in the format of table to detail how polysulfide are formed step by step.

Step 1. At the beginning of the discharge process, solid-liquid two-phase reaction can take place.

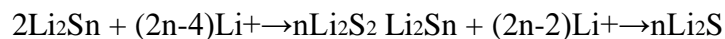
It is well established that sulfur in the cathode exists in the form of large molecules. To be specific, sulfur atoms tend to form various kinds of homoatomic chains or rings. Octasulfur (cyclo-S<sub>8</sub>) that can easily crystallize at room temperature and form orthorhombic architecture is the most stable allotrope of sulfur ever known. Therefore, transition from sulfur to Li<sub>2</sub>S cannot occur in one-step reaction. In the typical discharging process of a fresh lithium sulfur battery, Cyclo-S<sub>8</sub> is reduced and S-S covalent bond of ring-structural cyclooctasulfur S<sub>8</sub> is first broken, leading to the formation of soluble Li<sub>2</sub>S<sub>8</sub> with high polarity [34]. It is well known that the reduction product Li<sub>2</sub>S<sub>8</sub> can easily dissolve into organic electrolyte. So this step is accompanied with fast reaction kinetics.



Step 2 . Liquid-liquid one-phase reaction takes place. The formation of various order of lithium polysulfides with the general formula of Li<sub>2</sub>S<sub>n</sub> results from a series reduction from the dissolved Li<sub>2</sub>S<sub>8</sub>. The initially formed polysulfides have longer chains (4<n<8) and higher solubility in the electrolyte. With the length of the chains reducing, the voltage of the battery system gradually decreases and the viscosity of the electrolyte increases.



Step 3. In the later stages during discharge, liquid-solid two-phase reaction occur. The formerly dissolved long-chain polysulfides turn into short-chain polysulfides through reduction process. The formation of insoluble Li<sub>2</sub>S<sub>2</sub> results from the deposition of polysulfides. This process leads to an insulating passivation layer on the surface of the electrode and a significant increase in the internal resistance of the LSB system. Since the solid nucleation requires a large amount of energy, so this conversion is hard to occur.



Step 4. Solid-solid one-phase reaction occur. In the final step of the discharging,  $\text{Li}_2\text{S}_2$  is reduced to  $\text{Li}_2\text{S}$ . Since the solid environment hampers the flexible diffusion of lithium, so this conversion is the most difficult one [35,36]. There is no following possible reduction of sulfide ions at this point, which is represented by the drastic voltage drop in the discharging profile. The capacity decay of LSB during the repeated charge-discharge cycling process mainly results from the loss of active material that occurred in this step.



From the illustrated figure, it can be seen that there are two noticeable discharging plateaus at the electrochemical potential of 2.3V and 2.1V with liquid ether-based electrolyte. The very first voltage plateau of discharging curve represent the conversion of  $\text{S}_8$  and formation of high-order polysulfides. The stepwise region between both plateaus is often attributed to the formation of medium-order polysulfides such as  $\text{Li}_2\text{S}_4$ . The second plateau corresponds to the reduction of  $\text{Li}_2\text{S}_4$  and the formation of  $\text{Li}_2\text{S}$ .

## 2.2 Technical issues and challenges for LSB

Despite a number of desired merits (high natural abundance, an inherently low competitive cost, non-toxicity, considerably high theoretical specific capacity) of the rechargeable lithium sulfur battery system make it appealing to scientists and researchers and give it overwhelming advantages against other former counterparts. There is no denying that three major challenges associated with three key constituents of the lithium sulfur battery have to be addressed to fulfill technical improvement, extensive utilization and future commercialization in the market. The limitations and challenges of overall high

performance of LSB result from different cell components. A concise and comprehensive description is shown below.

### 2.2.1 Lithium metal anode (negative electrode)

Lithium metal has been the most frequently used material for the anode in the past few years due to the desired attributes (low reduction potential, low density, extraordinarily high theoretical specific capacity). Four daunting drawbacks (non-uniform electrodeposition, volume expansion, unstable solid electrolyte interphase and) have significantly limits the performance of the lithium sulfur battery system. Serious safety issues like explosion and complete cell death can be provoked by those aforementioned problematic aspects. Although massive amount of attempts have been undertaken to find a proper solution, it still remains as an unresolved problem of metal lithium anode. These four are persistent problems associated with lithium metal anode and will be briefly interpreted and schematically shown in Figure 2-4.

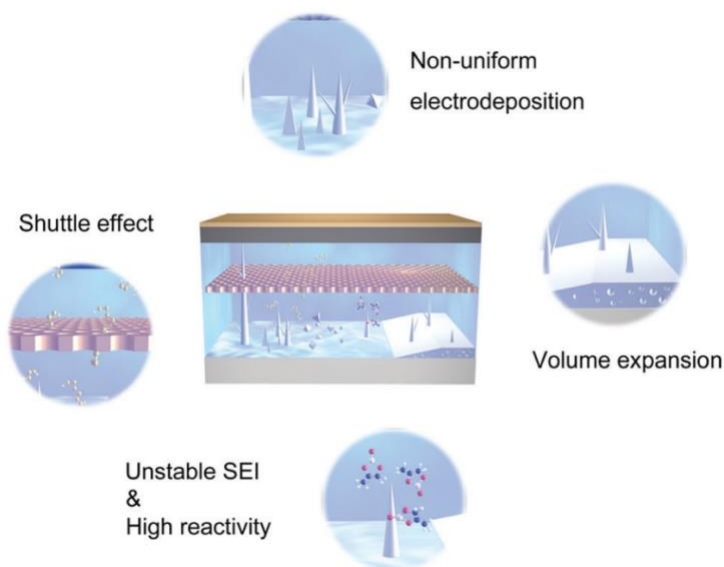


Figure 2- 4 The typical issues that lithium metal anode face [37].

First of all, the substrates' uniformity (the surface of the anode and solid electrolyte interphase) and the concentration gradient of ions can determine the nucleation rate of dendrite particles [38]. For instance, ionic charges distribute unevenly on the surface of the anode depending on the surface roughness and fast lithium deposition can easily occur on the sharp tips of the substrate owing to the concentration gradient. The uneven lithium deposition can lead to intensified surface roughness in the first place and further result in more dendritic.

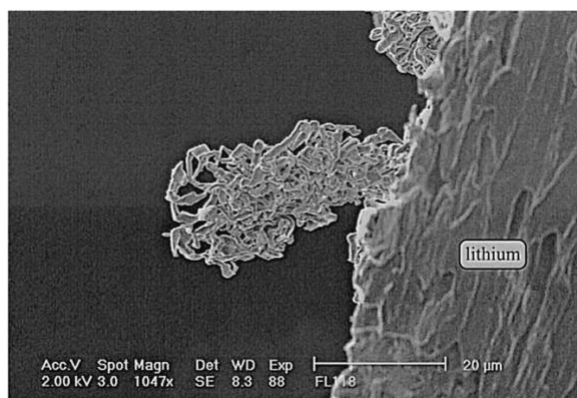


Figure 2- 5 Lithium dendrite formation in a lithium battery [39].

It is well acknowledged that long sharp dendrites schematically illustrated in Figure 2-5 can easily poke the polymer-based separator and result in severe outcome, which is explosion. Second of all, it is well known that there is a huge distinction between carbon- based anode in lithium ion battery and lithium metal anode in lithium sulfur battery. Porous carbon-based anode is merely used as a scaffold for ion intercalation and does not get involved in complicated redox. However, metallic lithium has to go through a complex stripping/plating process during the charge/discharge process and is not a suitable matrix for ionic electrodeposition. Thus, the morphological architecture has to undergo a significant change and is unable to control [40]. Eventually, the increased volume of the lithium metal anode from a charged state to a discharged state can give rise to irreversible destruction of solid electrolyte interphase. Thirdly, the dense and compact solid electrolyte interphase layer is formed by

spontaneous reaction between metallic lithium and organic electrolyte in the first several cycles [41]. Solid electrolyte interphase comprised of polymer-based material is of great importance due to its ability to impede reaction between electrolyte and anode and prevent loss of active material. Some severe issues that solid electrolyte interphase face are that parasitic crack forms on the surface and the dense layer needs to be reconstructed, which can lead to reaction between metallic lithium and electrolyte and huge consumption of active materials. Last but not least, the shuttling effect is caused by the dissolution of the intermediate sulfur products in the electrolyte and diffusion of soluble polysulfide to the metallic lithium anode. The cracks formed on the solid electrolyte interphase make the compact layer quite fragile and easy to break. The pristine lithium embedded in the deeper layer will be exposed and reacting with the sulfur intermediate products, leading to further consumption of active material.

### 2.2.2 Electrolyte

Under normal condition, electrolyte is composed of multiple organic solvents and metallic lithium salt in the case of lithium sulfur battery. Two key components will be briefly described and schematically illustrated in Figure 2-6. Polysulfide anions and anionic polysulfide radicals can get involved in a variety of reactions such as redox and radical reaction.

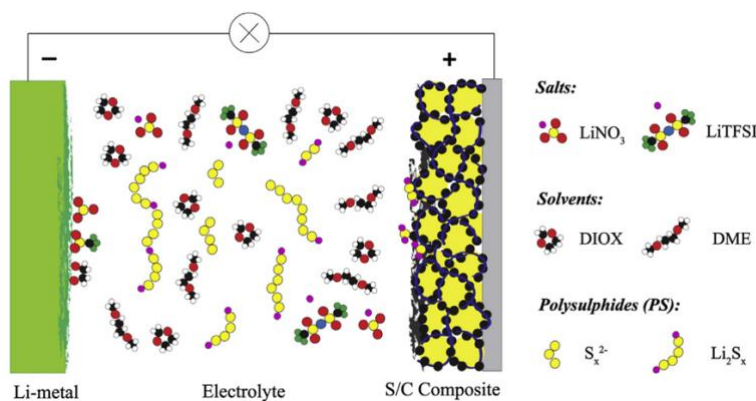


Figure 2- 6 Schematic diagram of components of a typical lithium sulfur battery with electrolyte consisting of lithium salts [42].

It is well established that polysulfide is reactive with ester, phosphate, carbonates, which are commonly used electrolyte solvents [43]. However, in the specific case of lithium sulfur battery, researches have shown that linear and cyclic ethers turned out to be the optimal solvents, such as dimethyl ether (DME) and 1,3-dioxolane (DOL). DME and DOL has their own merits and drawbacks. When cyclic DOL is used, the stronger SEI is formed on the surface of the anode, but polysulfide is poorly dissolved and polysulfide has sluggish reaction kinetics. When linear DME is utilized, polysulfide is fully dissolved and it has extremely fast reaction kinetics, but consumption of lithium metal happens due to reaction between DME and lithium. Enhancement in specific capacity and capacity retention can be done by using the combination of cyclic DOL and linear DME [44]. Even if the parasitic shuttle effects result in so many severe outcomes, the lithium sulfur battery is unable to function perfectly without the dissolution of polysulfide in the electrolyte. To be specific, cyclo-S<sub>8</sub> can only be reduced on the interface of sulfur and carbon without polysulfide dissolving in the electrolyte. The fresh sulfur embedded in the deeper layer cannot be used, which leads to extremely low specific capacity. There always would be a tradeoff that needs to be taken into consideration. The solvent used in the liquid electrolyte has to satisfy some specific requirements. The following critical criteria shown below have to meet in the case of lithium sulfur battery system.

1. Has high chemical stability when directly contact with lithium metal anode and polysulfide species.
2. Can provide high polysulfide solubility.
3. Offers poor viscosity for polysulfide solution.

Extensive effort has been done to find the most desired organic solvent for the rechargeable lithium sulfur battery in the past few decades and different types of seemingly suitable organic solvent have been experimented through the scientific research. Eventually, a great number of publications have stated that linear and cyclic ethers are the most desired organic solvent, on top of that, a specific ratio



of DOL and DME, which is 1 : 1, is the most suitable recipe of the organic solvent according to the scientific community.

As a critical component of the electrolyte, lithium salt ought to satisfy some certain requirements. High chemical and electrochemical stability of the anion are required and the salt has to be highly dissociative in the electrolyte solvent. There is no denying that lithium salt can provide a huge amount of dissociated positive lithium ions moving freely in the electrolyte. But a significant balance has to be taken into account. The capacity of constructing a compact thin film on the anode and the ability to prevent oxidation on the cathode to occur are both crucial for the battery system [42]. The most extensively used lithium salt is LiTFSI for lithium sulfur battery due to its remarkable thermal stability. Initially, an unpleasant issue arose, which was that the aqueous solution of lithium-based salt was highly reactive with the polysulfide formed during the discharging process. Considerable researches have been conducted to find the solution to the issue. Eventually, a number of publications have clarified that the daunting issue can be resolved by lithium-based salt dissolving into the ether-based organic solvent. The most suitable lithium salt, LiTFSI, turned out to be greatly compatible with ether solvents. Another significant component that has to be mentioned is lithium salt additive. Not many researches have been done and this area is still in the infancy and full of mystery to explore. But undoubtedly, additives play a significant role in the functional electrolyte and a small amount of additive is enough to make a big difference in the performance of the battery system. The most frequently utilized example is  $\text{LiNO}_3$ .

### 2.2.3 Sulfur-based cathode (positive electrode)

It is well known that sulfur is a yellow solid nonmetal and has more than 30 different allotropic forms. Sulfur in the cathode exists in the form of large molecules. To be specific, sulfur atoms tend to form various kinds of homoatomic chains or rings. Octasulfur (cyclo- $\text{S}_8$ ) that can easily crystallize at

room temperature and form orthorhombic architecture is the most stable allotrope of sulfur ever known, having a molecular weight of 32.066 g mol<sup>-1</sup> and having a density of 2.07 g cm<sup>-3</sup>. Sulfur is the seventh most abundant element on the earth and its purification techniques are very simple. Sulfur has a relatively low melting point of 115°C and can be easily sublimed. The very first sulfur dry cell was developed in the early 60s. However, sulfur-based battery was not extensively investigated and used in the next 40 years due to its complicated principle of chemistry. With the rapid development of science and technology, lithium sulfur battery has regained the attention. Lithium sulfur battery is still in the infancy even though it has been investigated for a few decades. A few challenges and drawbacks associated with sulfur-based cathode impeding the commercialization of lithium sulfur battery are listed below:

1. Polysulfide shuttle effect
2. Insulating property of sulfur
3. Volume expansion
4. Self-discharge Polysulfide shuttle effect

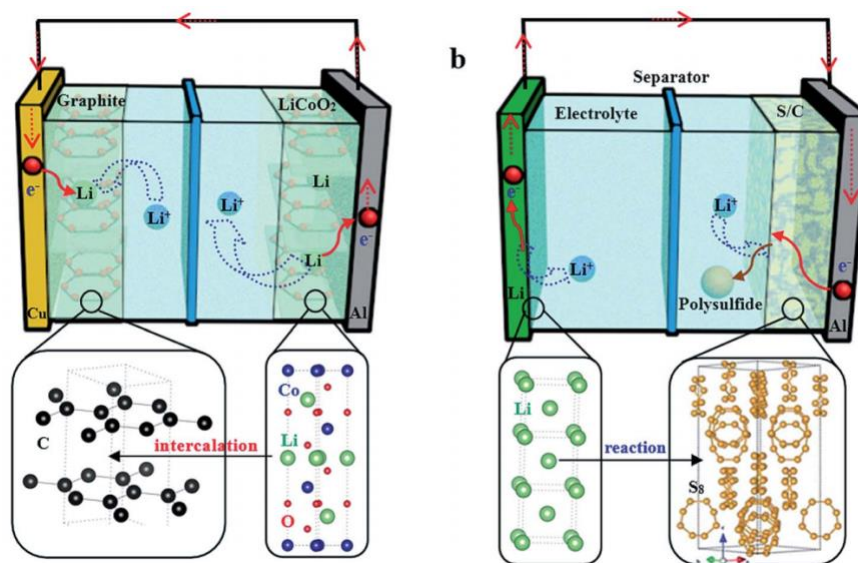


Figure 2- 7 A schematic illustration of the working principles of (a) graphite/LiCoO<sub>2</sub> lithium-ion battery and (b) lithium-sulfur battery [45].

As schematically illustrated in Figure 2-7, reversible conversion of lithiation and de- lithiation are the main reactions in lithium ion battery and the performance of the battery highly depends on the capacity of transporting lithium ions back and forth between anode and cathode [46-47]. There is a huge distinction in working principle between LIB and LSB. A series of intermediate sulfur products are produced through a series of redox reaction during charge- discharge process. Polysulfide dissolving in common organic electrolytes used for LSB is a very challenging issue. These intermediate products generated during the continuous reduction reaction tend to dissolve into ester-based electrolyte during the reaction. They have strong tendency to migrate through the polymeric separator and reach the lithium metal anode where they are further reduced to insoluble  $\text{Li}_2\text{S}$ , causing irreversible loss of active materials and creating passivation on the surface of metallic lithium anode via deposition of insoluble lithium sulfide [48-49]. Therefore, this continuous conversion of intermediate sulfur products has a negative impact on the overall performance of lithium sulfur battery. There is an urgent need to address this serious problem to scale up the production of LSB.

***Insulating property of sulfur:*** It is well known that the overall performance of lithium sulfur battery highly depends on the ability of transportation of charged lithium ions between anode and cathode. However, high performance of the battery is greatly hampered by the non-conducting nature of elemental sulfur. Despite the rapid solid-liquid conversion kinetics, fulfilling the theoretical capacity of  $418 \text{ mAh g}^{-1}$  is very difficult in the upper discharge plateau. sulfur still remains unreacted despite undergoing a number of charge-discharge cycles [50]. Extensive effort has been done to address this formidable challenge and an effective approach that was put forward by the scientists was that it is necessary to add conducting additive into the sulfur-based cathode. Significant enhancement in conductivity can be achieved by adding porous carbon materials, polymer derived carbonaceous material, metal oxides and organic metal framework. The main goal of these technological methods is to lower the amount of non- active material as much as possible and maximize the mass of active material

to achieve the maximization of practical energy density [51].

**Volume expansion:** Volume expansion is one of the main obstacles hindering the high performance of lithium sulfur battery. In the case of lithium ion battery, only approximately 20% of the total volume undergoes irreversible expansion. Unlike LIB, at least 80% of the overall volume go through formidable expansion, leading to rapid capacity decay and low coulombic efficiency.

**Self-discharging:** Figure 2-8 associated with self-discharging is shown below. Like traditional nickel- cadmium battery, lithium sulfur battery exhibits parasitic self-discharging behavior.

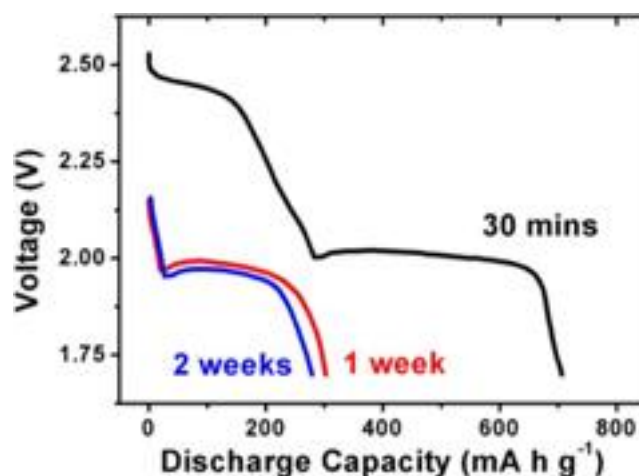


Figure 2- 8 Schematic diagram of self-discharging at different periods [18].

Moreover, many studies have shown that conventional organic solvents such as carbonate-based electrolyte have low compatibility with sulfur-based cathode. Intermediate sulfur species can easily dissolve into carbonated solvents and can be highly reactive with the traditional solvents, resulting in a significant decrease in capacity in the first few charge- discharge cycles. Massive work has been done to address this formidable problem. Ether-based solvents such as cyclic DOX and linear DME can be promising candidates for the solvents of electrolyte. They both are frequently used solvents in current research work. To further eliminate the parasitic self-discharging issue, solvents additives are added to enhance the overall performance of lithium sulfur battery.

## 2.3 Approaches to overcome the serious issues and challenges

A number of effective approaches have been attempted to circumvent the drawbacks and challenges to enhance the overall performance of lithium sulfur battery. These strategic methods can be classified into four main categories depending on the components: cathode modification, anode modification, electrolyte modification and separator modification. My work is mainly focused on the sulfur-based cathode modification, so different methods that are associated with cathode modification will be stated below.

### 2.3.1 Modification of sulfur-based cathode

#### 2.3.1.1 Synthesis of sulfur-carbon composite

Carbon performs double duties in the case of sulfur-carbon composite. It is not only used as scaffold to accommodate the sulfur species, but also used as conducting material to compensate the insulating nature of sulfur. It is commonly used due to its remarkable attributes such as low cost, abundance, high ionic and electronic conductivity and great inertness against continuous voltage alteration. A variety of strategic methods have been applied to synthesize the highly required sulfur-carbon composite. The various strategic approaches can be categorized into three groups depending on the mechanism of synthesis.

##### 2.3.1.1.1 Thermal treatment

Thermal treatment technology can be categorized into two sub-technologies: melt infusion and vapor deposition.

##### 2.3.1.1.1.1 Implementation of melt infusion

In the case of melt infusion, the basic principle is that elemental sulfur is heated to a certain temperature and let solid sulfur melt. The molten sulfur showing the lowest viscosity is able to diffuse

into the micropores of carbon spheres and get entrapped inside the microscopic pores. The set-up temperature is approximately 160°C, which is above the melting point of sulfur. Another distinct advantage is that sulfur exhibits its lowest viscosity at that temperature, which fastens the process of molten sulfur going to the microscopic pores embedded inside carbon. A number of productive researches regarding melt infusion method have been done.

Zhang et al. [52] reported that the thermal treated mixture of sublimed sulfur and carbon spheres has a strong capacity of entrapping sulfur into the pores of carbon spheres and constraining the electrochemical reaction inside the micropores, leading to remarkable capacity retention and exceptional reversibility. Porous carbon spheres with interconnected pore channels and large pore volume were synthesized to achieve a high sulfur loading, which is beneficial for excellent performance of LSB. In contrast to the conventional preparation of sulfur-carbon composite, the first step in their work is the dissolution of sucrose used as carbon source into aqueous solution containing sulfuric acid. The resultant black-colored products were collected by simple filtration and followed by the thermal calcination at elevated temperature under argon-filled atmosphere. The subsequent step is thermal treatment of mixture of obtained carbon spheres and commercial sublimed sulfur in a well- sealed container under argon-filled atmosphere. Significant improvement in sulfur encapsulation and exceptional confinement of soluble polysulfide diffusion have been accomplished by Zhang and his co-workers using melt infusion approach. Such a simple and controllable methodology to successfully achieve sulfur-filling and effectively accommodate the parasitic volume expansion during the repeated charge-discharge cycling process is attracting increasing attention. Furthermore, realization of shortened migration pathway for lithium ions and drastically increased electronic kinetics can be enabled by the extremely thin wall of carbon sphere, which is another appealing character for sulfur-carbon composite. The structural stability and enhanced electrical contact with active material sulfur can also be maintained and achieved by this innovatively designed sulfur-carbon composite. Some of his remarkable experimental results are

schematically shown in Figure 2-9.

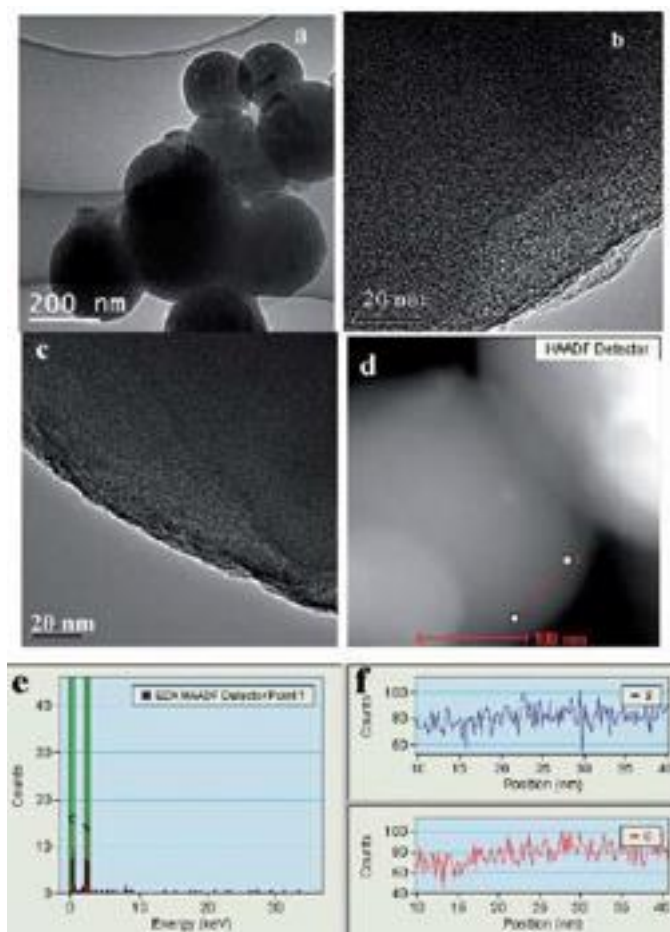


Figure 2- 9 Schematic diagram of TEM image of carbon sphere (a,b) and sulfur-carbon composite (c) high-angle annular dark field-scanning TEM image (d) EDX spectrum (e) corresponding line scans [52].

Xin et al. [53] reported that a novel and innovative design of metastable small sulfur molecules of S<sub>2-4</sub> constrained in a highly conducting microporous carbon host is an effective approach to prevent huge loss of active material, diminish the fast capacity fading and improve the poor electronic conductivity of sulfur. In contrast to the conventional preparation of sulfur-carbon composite, in this work, the very first step of synthesis is incorporation of multiwalled carbon nanotubes with an average diameter of approximately 50 nm and mesoporous carbon via a solution-based method. A coaxial structure with a core of CNT and a protective MPC sheath with a thickness of approximately 100 nm is

achieved. The subsequent step is melt infusion of mixture of metastable small molecules of sulfur allotropes  $S_{2-4}$  and CNT@MPC where molten sulfur diffuses as chain-like molecules into the mesoporous carbon layer to form multifunctional sulfur-carbon composite. The composite undoubtedly exhibits highly improved cycling durability, capacity retention and significantly prolongs the span life of the battery. Some of her productive results are schematically illustrated in Figure 2-10.

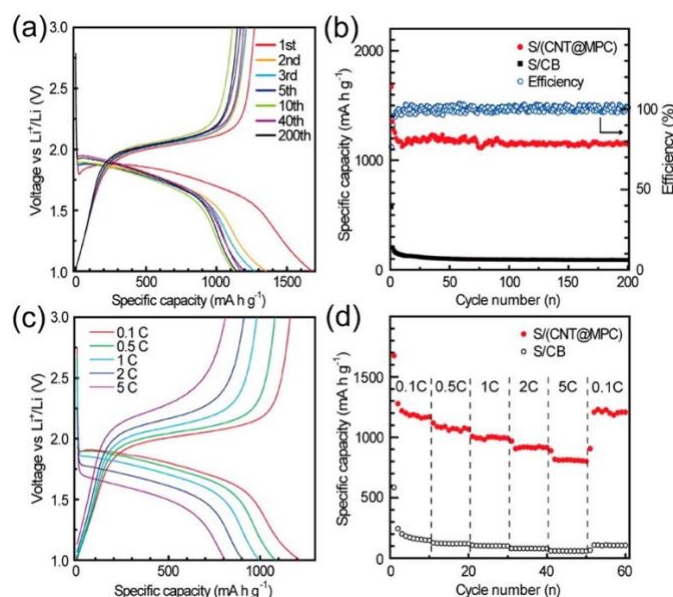


Figure 2- 10 Schematic diagram of electrochemical performance of S/(CNT@MPC) composite and comparison with traditional S/CB composite [53].

An innovative approach called pore-filling has been proposed by Ji and his co- workers [54]. In contrast to the conventional preparation of carbon-sulfur composite, the first step in their work is fabrication of CMK-3 using SBA-15 with size-controlled short-rod morphological structure as hard template through a nano-casting approach. To be specific, as-synthesized SBA-15 was dissolved into sucrose-containing sulfuric acid solution and the obtained mixture was vigorously stirred and was followed by the thermal treatment. The additional impregnation process was performed with the extra addition of sucrose-containing sulfuric acid solution. After the thermal carbonization under argon-filled atmosphere, the removal of SBA-15 hard template was performed by vigorously stirring in aqueous



solution containing hydrofluoric acid. The subsequent step in their work is preparation of CMK-3/S multifunctional nanocomposites through a melt-diffusion strategical method. Basically, the ground fine CMK-3 particles and sulfur particles were thermally treated at certain temperature. The tunable weight ratio of sulfur/carbon plays a pivotal role in accommodation of formidable volume expansion during charge-discharge. The volume expansion and volume contraction can be effectively tuned by the channels that mesoporous carbon provides. The interconnected pore structures are formed from carbon tubes and ensure readily absorption of sulfur into their pores. The synthesis of the composite can be done by infiltration of elemental sulfur into the mesoporous structure of carbon. It is crucial to physically tailor the microscopic structure of cathode to meet high criteria of successfully hindering dissolution of soluble polysulfide species and perfectly retaining the ionic and electronic conductivity. Pore-filling along with mesoporous carbon architecture is full of great practical promise for lithium sulfur battery application. Some of the productive results are schematically illustrated in Figure 2-11 and Figure 2-12.

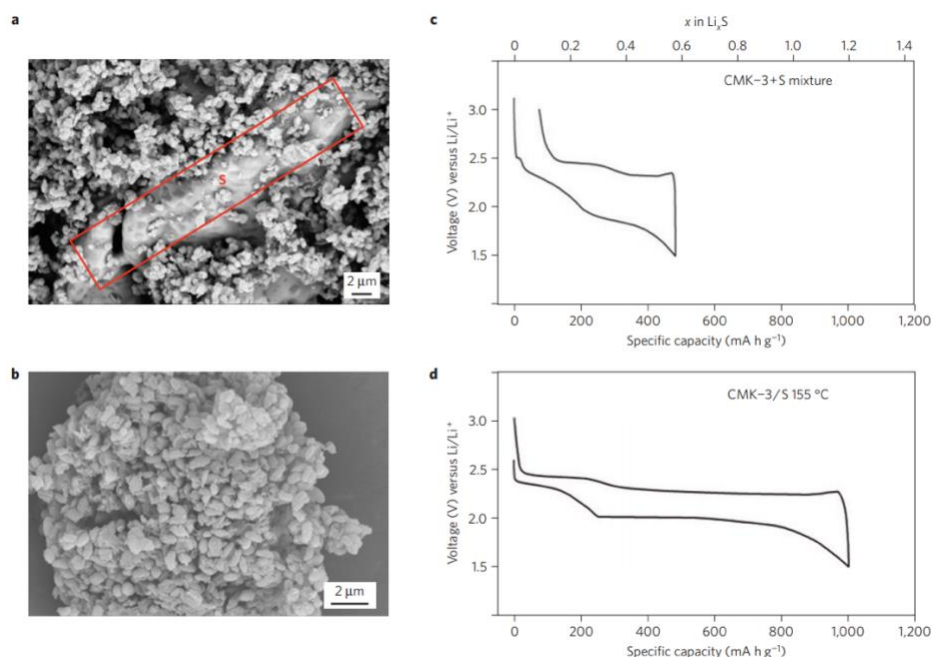


figure 2- 11 SEM images of CMK-3/S and its electrochemical performance. a, CMK-3/S before thermal treatment. b, thermally treated CMK-3/S at 155 oC, demonstrating that elemental sulfur disappears. c,d, comparison of galvanostatic charge-discharge curves between CMK-3/S with heating and CMK-3/S without heating [54].

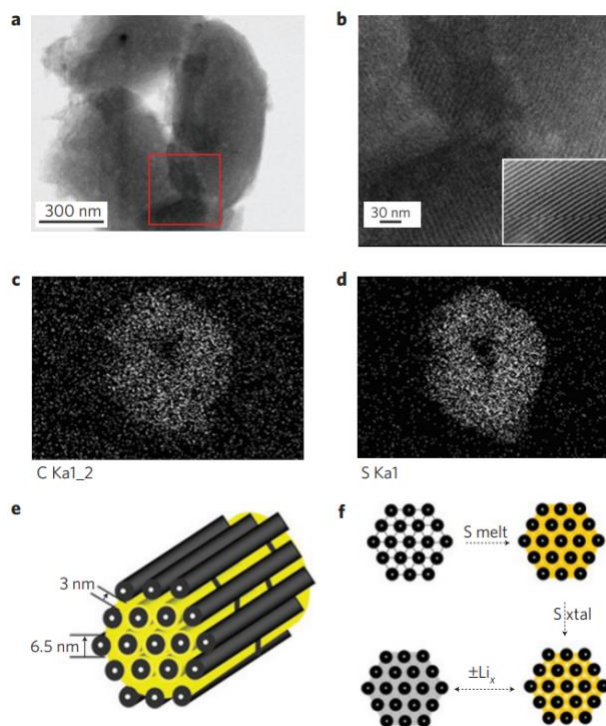


Figure 2- 12 a, CMK-3/S heated at 1550°C b, magnified image c,d, uniform distribution of sulfur and carbon e, schematic diagram of elemental sulfur constrained in the highly ordered interconnected pores of CMK-3 f, schematic diagram of the process of composite synthesis [54].

Zheng et al. [55] reported that successful hinderance of free diffusion of polysulfides and effective impedance of rapid capacity fading can be accomplished by introduction of hollow carbon nanofiber-encapsulated sulfur cathode. Andic aluminum oxide (AAO) templates are utilized to fabricate hollow carbon nanofiber array by the approach of thermal carbonization of polystyrene. The fabricated hollow nanofiber array performs two essential duties of inhibition of sulfur coating onto the outer wall of hollow carbon nanofibers and facilitation of sulfur infusion into hollow carbon nanofibers. This fabricated hollow nanofiber array is excellent for entrapment of soluble intermediate sulfur species, successful accommodation for volume expansion of sulfur during charge-discharge process and faster transportation of lithium ions. To be specific, the hollow carbon nanofibers with excellently high-aspect-ratio can successfully confine sulfur inside of them and effectively limit the contact between sulfur and

the electrolyte to only two openings. The large space that the hollow carbon nanofibers provide play a pivotal role in accommodating the formidable volume expansion of sulfur during charge-discharge cycling process. Realization of fast ionic transportation can be achieved by lithium easily penetrating the ultra-thin carbon wall. In contrast to conventional preparation of sulfur-carbon composite, the first step in their work is dropping mixture of polystyrene (PS) and dimethylformamide (DME) onto the AAO template to obtain the carbon precursor. The subsequent step is thermal carbonization by heating the mixture of AAO/PS/DME at elevated temperature to obtain carbon-coated AAO template. Subsequently, the heat-treated AAO template was loaded into a small vial with the addition of 1% sulfur suspended in toluene solution. This simple and facile strategic approach exhibits exception results compared to conventionally prepared sulfur-carbon composites and successfully accomplishes high cycling stability and provides extremely high specific capacity. Some of the productive results are schematically illustrated in Figure 2-13.

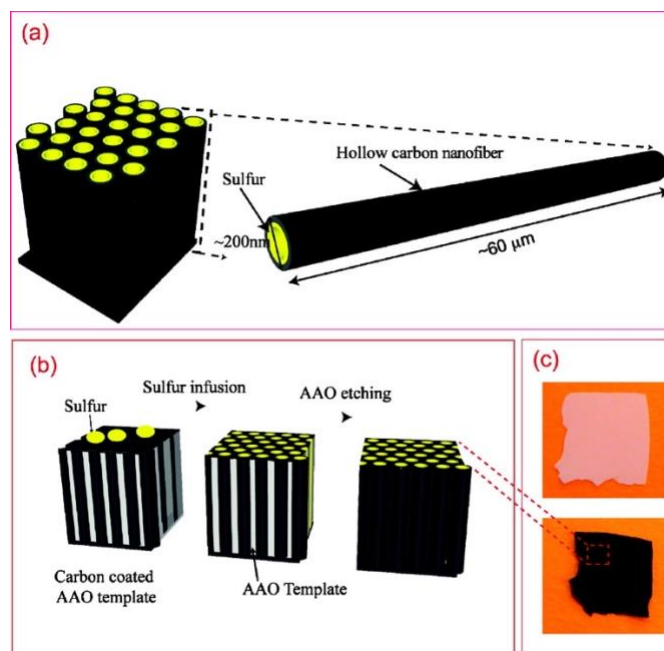


Figure 2- 13 Schematic diagram of fabrication of hollow carbon nanofiber/sulfur composite through melt infusion. (a) the high aspect ratio of hollow carbon nanofiber array (b) fabrication process of hollow carbon nanofiber array/sulfur composite (c) before and after carbon coating and sulfur infusion [55].

Zhang et al. [56] reported that the novel and rational design of double-shelled hollow carbon spheres is an excellent method to successfully confine sulfur lithiation reaction. Such sophisticated nanostructures perform multiple essential duties, such as effective suppression of soluble polysulfide dissolution, entrapment of extremely high loading mass of active material, provision of migration pathway for rapid ionic transportation, splendid mechanical stability, remarkable capacity of withstanding volume expansion during repeated charge- discharge cycles. In contrast to the conventional preparation of sulfur-carbon composite, the first step in their work is that highly porous SnO<sub>2</sub> hollow spheres evenly coated with glucose-derived polysaccharide on the outer and inner surfaces are utilized to prepare double-shelled hollow carbon spheres via the approach of thermal carbonization under hydrogen/nitrogen gas environment. What's more, double-shelled hollow carbon spheres can be produced by the simple dissolution of Sn particles obtained from the reduction of SnO<sub>2</sub> through thermal carbonization into hydrochloric acid, which accurately copy the morphological structure of SnO<sub>2</sub> hollow spheres. The main goal of the subsequent impregnation of sulfur performed at elevated temperature is to make the infusion of sulfur into the double-shelled hollow carbon spheres easier and accomplish superb entrapment of sulfur. The fabricated sulfur/carbon composite undoubtedly exhibits highly improved cycling durability, capacity retention and significantly prolongs the span life of the battery. Some of the productive results are schematically illustrated in Figure 2-14.

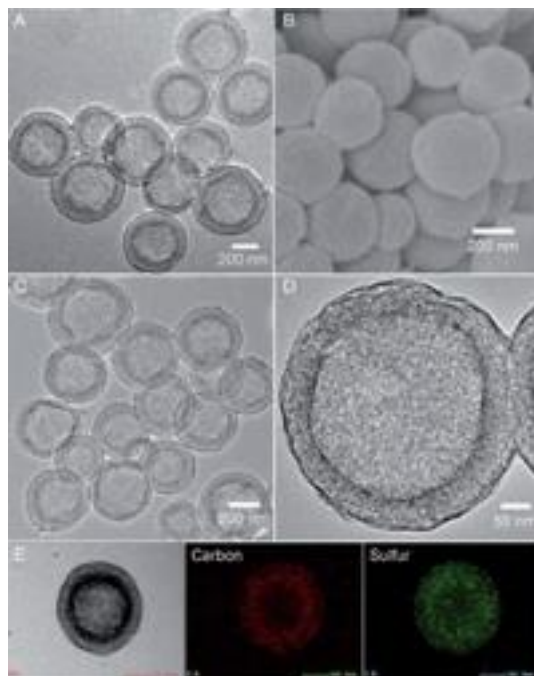


Figure 2- 14 (a) TEM image of DHCS (b) FESEM image of DHCS-S composite (c) and (d) TEM images of DHCS-S composite (e) EDX showing the elemental distribution [56].

Wang et al. [57] reported that the significantly improved overall performance of lithium sulfur battery was accomplished by the development of a microporous-mesoporous carbon with graphite architecture. The beneficial integrated structure has received tremendous amount of attention due to its amazing properties. The micropores can be suitable spots for constrained sulfur lithiation. The mesopores offer a migration pathway for ions and facilitate the rapid transportation of ions. The graphite structures undoubtedly have low internal impedance and excellent conducting nature for ions and electrons. In contrast to conventional preparation of sulfur-carbon composite, the first step of preparation is thermal carbonization applied in the mixture of phenolic resin solution and nickel hydroxide suspension. The subsequent step is elimination of metal species inside of the heat-treated mixture by hydrochloric acid etching. Subsequently, the selective extraction of sulfur from as-prepared CS-Ad powder was implemented by washing and filtering. Selective introduction of sulfur was done by the approach of melt adsorption-solvent extraction. This simple and facile strategic approach exhibits exception results

compared to conventionally prepared sulfur-carbon composites and provides extremely high specific capacity and excellent cycling stability. Some of the productive results are schematically illustrated in Figure 2-15.

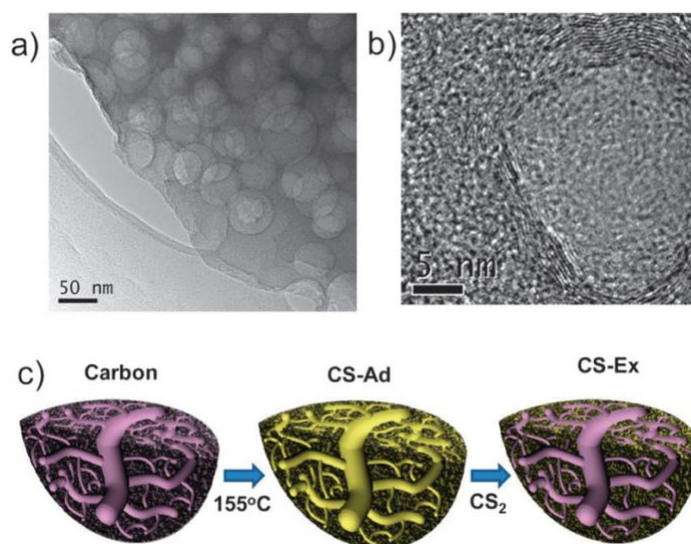


Figure 2- 15 (a) TEM image of carbon matrix (b) magnified TEM image of graphitic structure (c) schematic illustration of melt adsorption-solvent extraction [57].

#### 2.3.1.1.1.2 Application of vapor deposition

In the vapor deposition process, elemental sulfur is heated to a certain degree and becomes vaporous sulfur. Mesoporous carbon matrix can be excellent spots for vaporous sulfur deposition, leading to constrained sulfur lithiation and effectively hindered polysulfide dissolution. It is well known the boiling temperature of sulfur highly varies depending on the pressure. Vaporization temperature decreases with decreasing pressure.

Jayaprakash et al. [58] reported that the combination of template-based synthesis of mesoporous carbon particles and vapor infusion of sulfur into the pores is an inexpensive and facile method to fabricate excellent-performance lithium sulfur battery. In contrast to the conventional preparation of sulfur-carbon composite, the first step in their work is thermal decomposition of a low-cost carbon-

containing precursor (pitch) evenly deposited onto highly porous metal oxide nanoparticles to form carbon spheres. Subsequently, the well- shaped mesoporous hollow carbon spheres were obtained by simple and facile dissolution of the nanoparticle support. In other words, highly porous silica templates are utilized to prepare mesoporous hollow carbon spheres via the approach of thermal calcination under inert gas environment. The subsequent infiltration of sulfur was performed through vapor phase infusion. Ultra-high mass loading of sulfur can be realized by simply exposing the prepared porous carbon nanoparticles to sulfur vapor. The prepared carbon hollow spheres after heat treatment perform multiple crucial duties. They offer remarkable mechanical stability for vaporous sulfur infusion and provide exceptional migration pathway for ions. The fabricated sulfur/carbon composite undoubtedly exhibits highly improved cycling durability, capacity retention and significantly prolongs the span life of the battery. Some of the productive results are schematically illustrated in Figure 2-16.

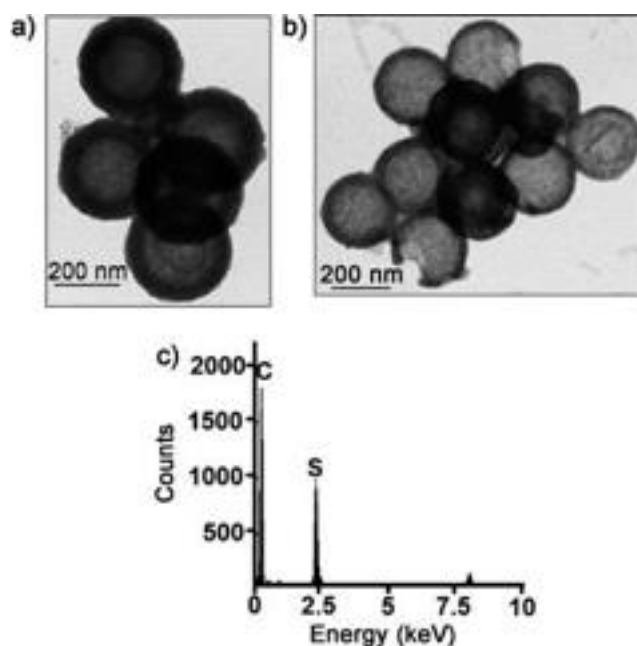


Figure 2- 16 (a) TEM image of mesoporous carbon hollow spheres (b) prepared carbon/sulfur composite (c) schematic illustration of EDX showing the distribution of sulfur [58].

Guo et al. [59] reported that a novel and innovative design of impregnation of sulfur into

disordered carbon nanotubes (DCNTs) is an excellent methodology to alleviate the serious problem of soluble polysulfide species dissolution. Incorporation of sulfur into mesoporous carbon host architecture to suppress polysulfide dissolution is the most promising physical confinement methodology. It provides so much more advantages over conventional physical confinement using barrier material. The template-based method was implemented to fabricate disordered carbon nanotubes. The anodic aluminum oxide membranes used as standard templates underwent the wetting procedure first, and then followed by thermal carbonization at high temperature under vacuum environment. The incorporation of vapor phase sulfur into the mesoporous carbon host structure was carried out at different temperatures to determine if varying temperature is an essential factor. The synthesized carbon-sulfur composite with graphitic architecture perform multiple essential duties, such as effective suppression of soluble polysulfide dissolution, entrapment of extremely high loading mass of active material, provision of migration pathway for rapid ionic transportation, splendid mechanical stability, remarkable capacity of withstanding volume expansion during repeated charge-discharge cycles. Some of the productive results are schematically illustrated in Figure 2-17 and Figure 2-18.

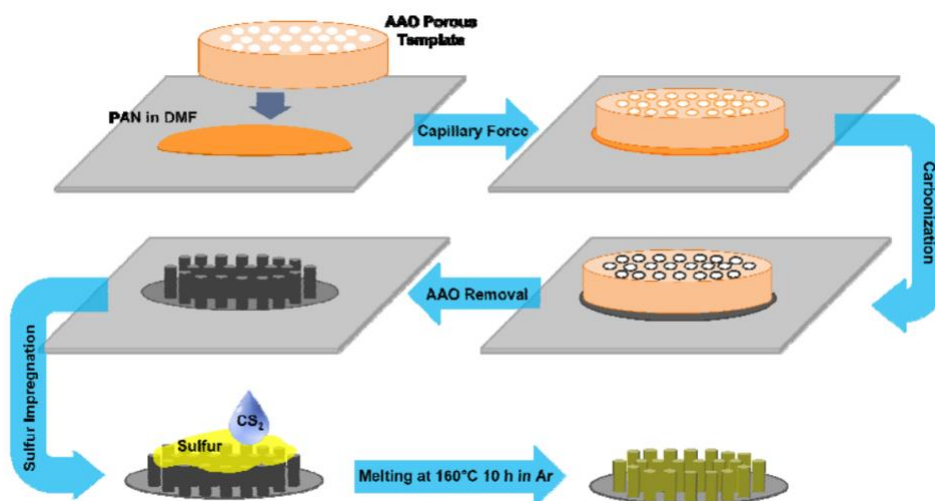


Figure 2- 17 schematic illustration of synthesis of sulfur-impregnated disordered carbon nanotubes [59].



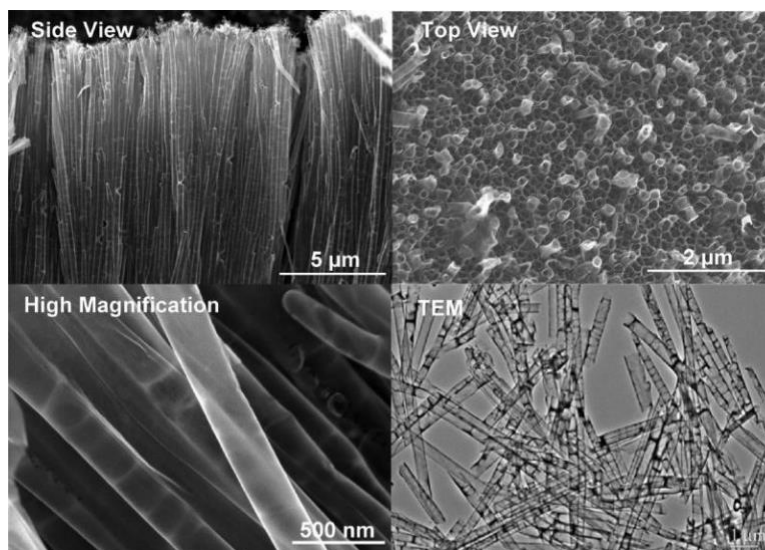


Figure 2- 18 SEM and TEM images of disordered carbon nanotubes through the approach of wetting technique [59].

Zhou et al. [60] reported that a novel and innovative design of self-supporting nanostructured sulfur-carbon composite is an excellent methodology to alleviate the serious problems that lithium sulfur battery face. This freestanding synthesized cathode has received tremendous amount of attention due to its excellent properties such as binder-free, remarkable ionic and electronic conductivity, exceptional flexibility. Another promising feature associated with this innovatively developed cathode material is that it does not have the metal-based current collector. The most commonly used anodic aluminum oxide template was employed to prepare mesoporous carbon host via the conventional thermal carbonization method. The impregnation of vapor phase sulfur onto the mesoporous carbon host structure is highly tunable. The synthesized carbon-sulfur composite with graphitic architecture perform multiple essential duties, such as effective suppression of soluble polysulfide dissolution, entrapment of extremely high loading mass of active material, provision of migration pathway for rapid ionic transportation, splendid mechanical stability, remarkable capacity of withstanding volume expansion during repeated charge-discharge cycles. The freestanding nanostructured composite tremendously prolongs the life span of

battery system and renders an excellent cycling stability. Another attracting aspect related to this innovatively designed membrane-based cathode is an ethanol evaporation-induced assembly technique. The sulfur-CNTs was dispersed in homogeneous ethanol solution and followed by ultrasonication for one hour. The evaporation of ethanol was carried out by heat treatment and flexible membrane was collected from the bottom of the container. Some of the productive results are schematically illustrated in Figure 2-19 and Figure 2-20.

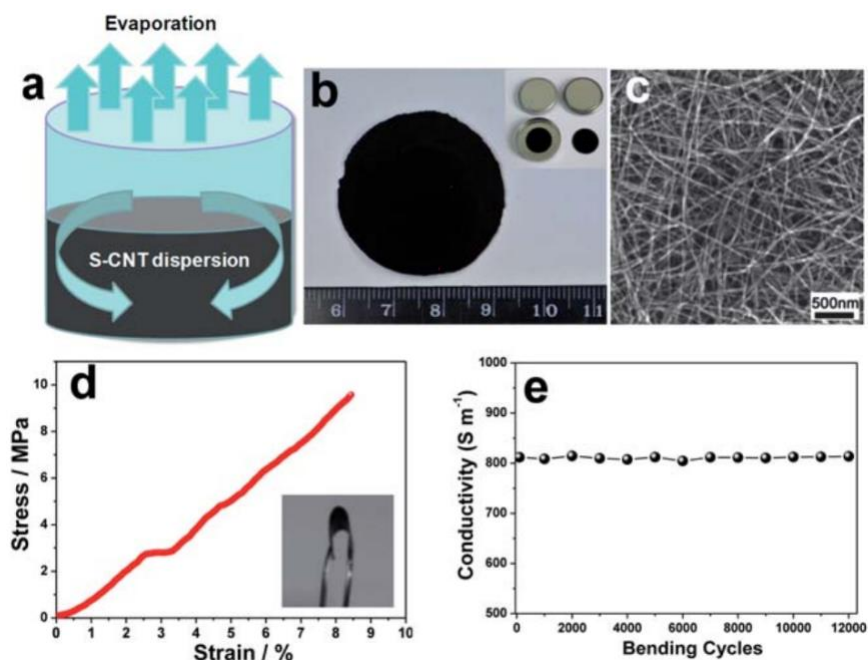


Figure 2- 19 (a) schematic diagram of assembly of membrane by the evaporation technique (b) S- CNT membrane (c) SEM image of S-CNT network structure (d) stress-strain curve of S-CNT (e) electrical stability of membrane [60].

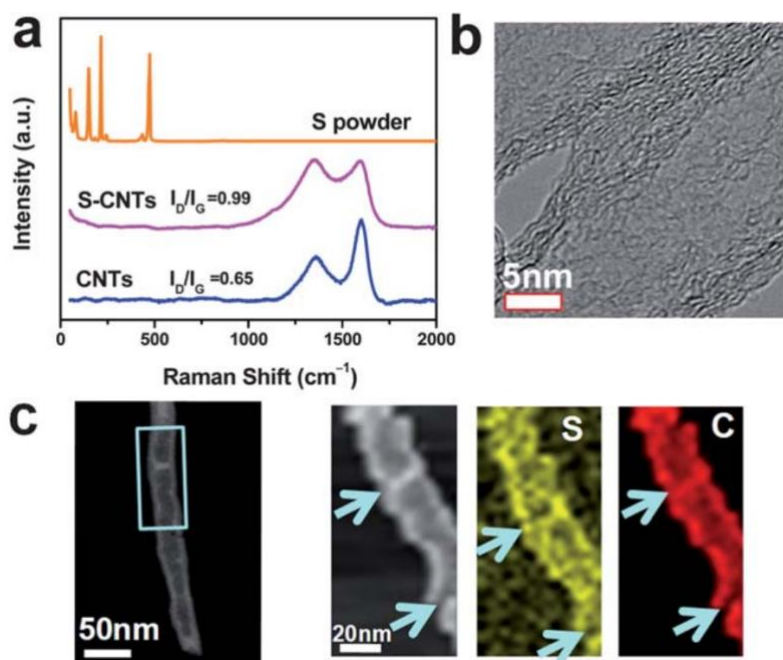


Figure 2- 20 (a) Raman spectra of CNTs, sulfur and S-CNT-23 (b) HRTEM image of microstructure of S-CNT-23 (c) STEM image of S-CNT-23 and elemental distribution [60].

#### 2.3.1.1.2 Chemical techniques

##### 2.3.1.1.2.1 Chemical precipitation

Elemental sulfur was prepared through chemical precipitation out of sulfur-containing compound. The most commonly used sulfur-containing compound is  $\text{Na}_2\text{S}_2\text{O}_3$  and the most frequently used acid is HCl. This inexpensive and environmentally friendly synthesis has received tremendous amount of attention from scientific community.

Although a significant amount of work has been focused on the encapsulation of active material into the mesoporous carbon hollow structures to effectively suppress the formidable polysulfide dissolution, relatively small amount of studies has been concentrated on another serious issue, volume expansion during lithiation process, leading to rapid capacity decay.

Seh et al. [61] reported that an innovative and novel design of nanostructured sulfur-  $\text{TiO}_2$  yolk-shell with massive inner void space is an excellent methodology to alleviate the severe issue of volume

expansion. In contrast to the conventional preparation of sulfur-carbon composite, the very first step in their work is the synthesis of size-controlled sulfur nanoparticles achieved by simply mixing HCl with aqueous polyvinylpyrrolidone-containing  $\text{Na}_2\text{S}_2\text{O}_3$  solution. The subsequent formation of  $\text{TiO}_2$  coating was achieved by simply adding concentrated ammonia and isopropanol to the previously obtained concentrated sulfur nanoparticles solution, which is followed by multiple addition of Titanium diisopropoxide bis(acetylacetonate) at an interval of 30 minutes. The collection of synthesized sulfur- $\text{TiO}_2$  core-shell morphological structure was implemented by simply washing through centrifugation to eliminate hydrolyzed  $\text{TiO}_2$ . Compared to bare sulfur and conventional sulfur- $\text{TiO}_2$  core-shell nanostructured particles, the innovative design of nanostructured sulfur- $\text{TiO}_2$  yolk-shell is so much more advantageous. The structural integrity of yolk-shell composite can be preserved during lithiation reaction by the massive inner void space. The nanostructured sulfur- $\text{TiO}_2$  yolk-shell composite renders the significantly prolonged span life of lithium sulfur battery, successfully limits the polysulfide dissolution and effectively accommodates the volumetric expansion during lithiation. Some of the productive results are schematically illustrated in Figure 2-21 and Figure 2-20.

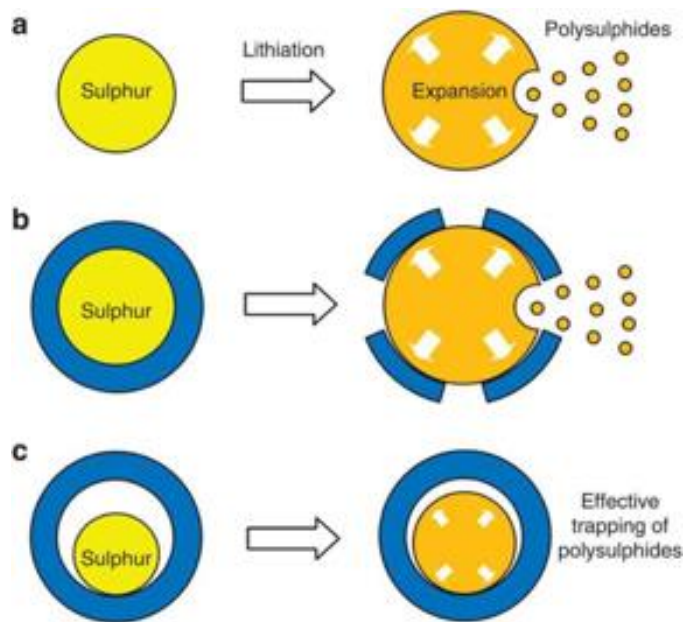


Figure 2- 21 (a) Fast capacity decay and low Coulombic efficiency can be induced by the parasitic dissolution of polysulfide species and volume expansion during lithiation process when bare sulfur particles are used in LSB system. (b) Even if the core-shell morphological structure offers a coating layer performing the protective duty. However, the cracks will still form on the surface of the shell when the core-shell goes through volume expansion during lithiation and the subsequent polysulfide dissolution will occur as well. (c) The yolk-shell morphological structure is much more advantageous than the conventional core-shell structure due to enormously large inner space, which can effectively accommodate the volume expansion during the lithiation process and can successfully maintain the structural integrity to realize effective entrapment of soluble polysulfide species [61].

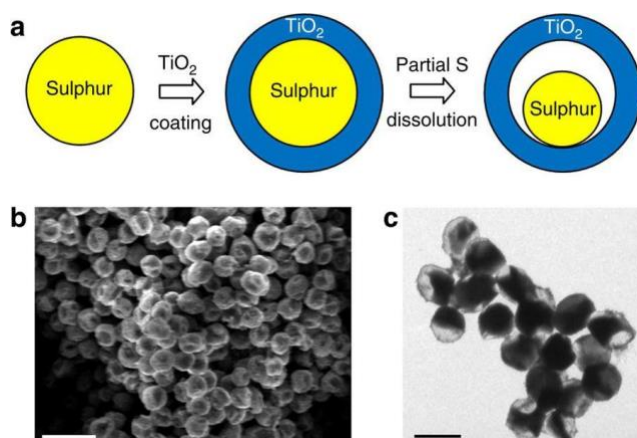


Figure 2- 22 (a) Schematic illustration of synthesis that consists of the formation of core-shell morphological structure done by coating the bare sulfur particles with  $\text{TiO}_2$  and the subsequent formation of the yolk-shell structure achieved by dissolution of sulfur in toluene (b) SEM images of fabricated yolk-shell morphological structure (c) TEM images of synthesized yolk-shell structure [61].

Park et al. [62] reported that their work is concentrated on an easy and inexpensive size-controlled sulfur particles synthesis through the mechanism of heterogeneous crystal growth. Sulfur particles with an average size of only a few microns are successfully grown in the inner spaces between randomly dispersed graphene sheets through a heterogeneous crystal growth mechanism. Suppression of impregnated sulfur particles growth is achieved by a graphene sheet with less than ten single graphene layers due to the limited interior interspace between layers. This innovative and novel synthesis performs appealing duties of accurately controlling the particle size of active material and affording composite powder in large quantities. In contrast to conventional preparation of sulfur-carbon composite, the first step of preparation in their work is mixing graphene powder and hydrofluoric acid to form active sites for sulfur particles to nucleate on the surface of graphene and to diminish the formidable impurities. The subsequent step is dispersion of HF-treated graphene into separately prepared  $\text{Na}_2\text{S}_2\text{O}_3$  solution by continuously stirring. Subsequently, realization of chemical precipitation of sulfur particles can be achieved with the addition of  $\text{H}_2\text{SO}_4$  into HF-treated graphene-containing  $\text{Na}_2\text{S}_2\text{O}_3$  solution. This method exhibits exception results compared to conventionally prepared sulfur-carbon composites and successfully accomplished high cycling stability, remarkable coulombic efficiency and almost no cyclic fading in the initial 50 cycles. Some of the productive results are schematically illustrated in Figure 2-23 and Figure 2-24.



Figure 2- 23 Schematic diagram of heterogeneous sulfur crystal growth mechanism [62].

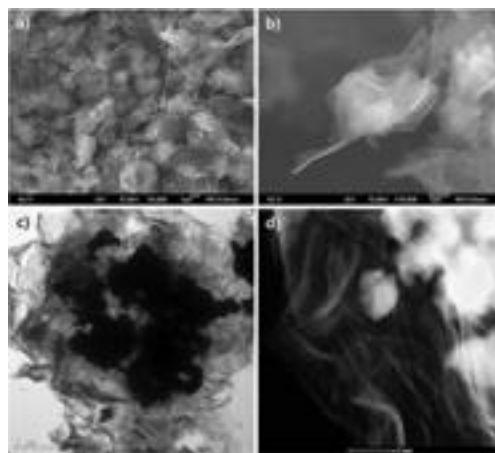


Figure 2- 24 (a) and (b) FESEM images of sulfur-impregnated graphene composite (c) and (d) bright filed TEM image and dark field TEM image of sulfur-impregnated graphene composite [62].

Su et al. [63] reported that an innovative and novel design of sulfur-multi-wall carbon nanotube (MWCNT) composite is an appealing methodology to realize the wide utilization of high-performance lithium sulfur battery system. These composite-based cathodes fabricated without binder and conventional metallic current collectors are so much more advantageous than any other traditional lithium sulfur batteries. Since the interwoven MWCNT network possesses remarkable self-weaving behavior, the key components such as binders and current collector are no longer required, leading to significantly simplified fabrication process and remarkably reduced weight. The first step of preparation of sulfur- MWCNT composite is separation of highly self-twisted MWCNT clusters with diluted solution of sodium thiosulfate ( $\text{Na}_2\text{S}_2\text{O}_3$ ), which is followed by simple ultrasonication along with the addition of isopropyl alcohol. The subsequent step is the incorporation of sulfur into intertwined multi-walled carbon nanotube achieved by simple addition of HCl into two separate previously obtained solution. These prepared sulfur-multi-wall carbon nanotubes perform multiple essential duties, such as effective suppression of soluble polysulfide dissolution, entrapment of extremely high loading mass of active material, provision of abundant migration pathway for rapid ionic transportation, abundant localized nano-scale reaction sites, splendid mechanical stability to withstand volume expansion during



repeated charge-discharge cycles. Realization of simple and facile binder-free and current collector- free fabrication process and elimination of environmentally hazardous effect of NMP can be accomplished through this promising design and development. Some of the productive results are schematically illustrated in Figure 2-25 and Figure 2-26.

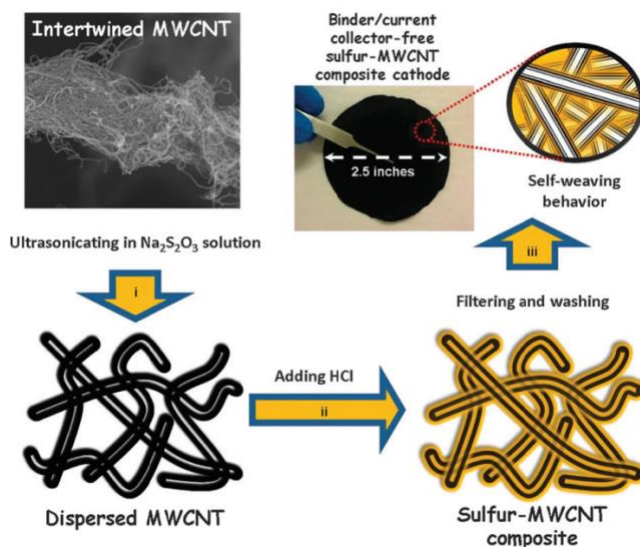


Figure 2- 25 Schematic diagram of fabrication of sulfur-MWCNT composite cathode [63].

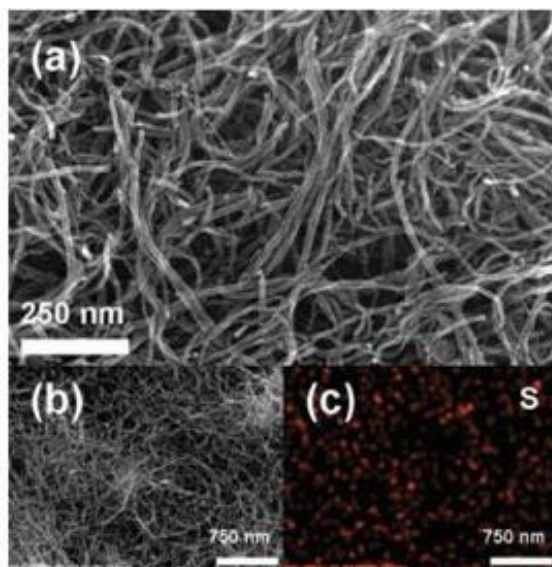


Figure 2- 26 (a) SEM image of interwoven MWCNTs (b) morphology of S-CNT-A sample (c) elemental mapping [63].



Wang et al. [64] reported that a novel and rational design and synthesis of graphene- sulfur composite by wrapping submicrometer sulfur particles with mildly oxidized graphene oxide sheets combined with carbon black particles along with PEG-containing surfactant in a simple manner. Elemental sulfur was gained by chemical precipitation out of sulfur- containing compound. The first step of the preparation of graphene-sulfur composite is the loading of carbon black particles onto graphene oxide with mild oxidation by bath sonication to improve the conducting performance of the mildly oxidized graphene oxide sheets. It is well established that mildly oxidized graphene oxide sheets possess hydrophilic functional.

Groups aiming at strongly bounding with water and hydrophobic functional groups aiming at forming strong bond with carbon black. The size-controlled sulfur particles are obtained by the PEG-containing surfactant, assuring that the size to the submicrometer scale. The introduced graphene-sulfur composite by coating the size-controlled sulfur particles with PEG-containing surfactant and mildly oxidized graphene oxide combined with carbon black nanoparticles perform multiple essential duties, such as effective suppression of soluble polysulfide dissolution, entrapment of extremely high loading mass of active material, provision of abundant migration pathway for rapid ionic transportation, abundant localized nano-scale reaction sites, splendid mechanical stability to withstand volume expansion during repeated charge-discharge cycles. Some of the productive results are schematically illustrated in Figure 2-27 and Figure 2-28.

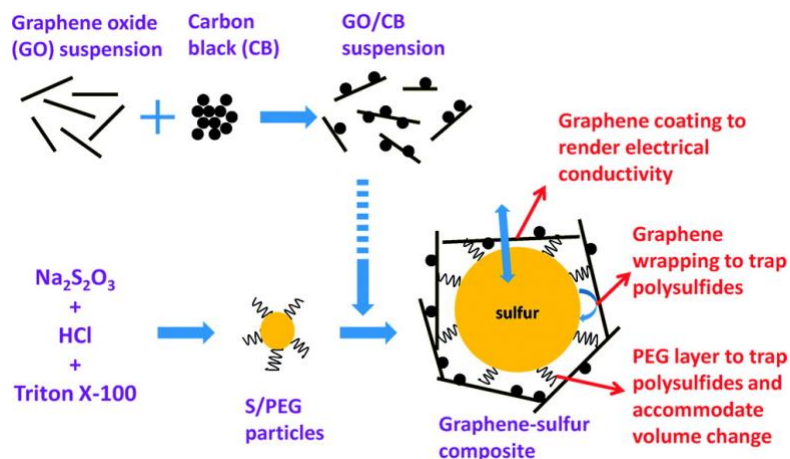


Figure 2- 27 Schematic illustration of synthesis of graphene-sulfur composite [64].

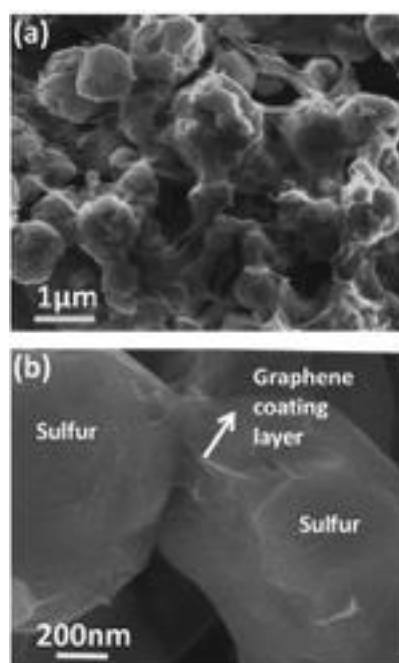


Figure 2- 28 SEM images of graphene-sulfur composite (a) at low magnification and (b) at high magnification [64].

Evers et al. [65] reported that an innovative and viable synthesis of graphene-sulfur composites exhibiting one of the highest sulfur loading mass (as high as 87%) is a scalable methodology for large-scale production of lithium sulfur battery. The innovative design has gained much more attention over

other batteries due to its appealing properties such as using simple one-pot preparation method, offering highly conducting wrap-like graphene for rapid ionic and electronic transportation. The elemental sulfur is gained by chemical precipitation out of sulfur-containing compound ( $\text{Na}_2\text{S}_x$  is used in this study). The first step of the preparation of graphene-sulfur composite is the mixing of graphene and soluble polysulfide. And the subsequent step is the implementation of oxidation in situ as a one-pot reaction. And then the synthesized composites were collected by filtration and washing. These synthesized graphene-sulfur composites perform multiple essential duties, such as effective suppression of soluble polysulfide dissolution, entrapment of extremely high loading mass of active material, provision of abundant migration pathway for rapid ionic transportation, abundant localized nano-scale reaction sites, splendid mechanical stability to withstand volume expansion during repeated charge-discharge cycles. Their appealing properties critically depends on highly conducting nature of graphitic structures and oxo-groups on the carbon surface, which highly facilitates polysulfides binding. Some of the productive results are schematically illustrated in Figure 2-29.

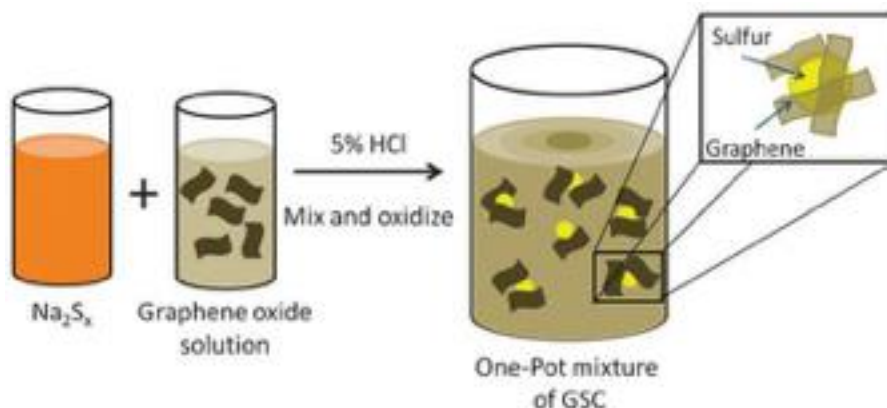


Figure 2- 29 Schematic illustration of one pot synthesis of graphene-sulfur composite [65].

#### 2.3.1.1.2.2 Solvent evaporation

Sulfur loading onto carbon nanotubes is achieved by dissolution of sulfur into organic solvents with high solubility and subsequent solvent evaporation. It is well known that cyclo- $\text{S}_8$  has orthorhombic

microstructure and its molecular structure is non-polar. This structural characteristic provides cyclo-S<sub>8</sub> high solubility into almost all kinds of organic solvents.

Hagen et al. [66] reported that a novel and rational design and synthesis of vertical aligned carbon nanotube/sulfur composites is an excellent methodology to alleviate the serious problems that lithium sulfur batteries face, aiming at large-scale production in the future. The synthesized CNT-sulfur composites are attracting more and more attention from scientific community due to its remarkable properties such as realization of one of the highest sulfur loading mass (as high as 70%) and significant decrease in weight along with tremendously simplified fabrication process owing to the absence of binder. In contrast to the conventional preparation process of sulfur-carbon composite by mixing and slurry coating, the first step of preparation in this work is the production of vertical aligned carbon nanotube through the approach of chemical vapor deposition on metal-based substrates. This step consists of two sub- steps. First of all, the deposition of catalyst thin film on metallic substrate is carried out by the method of chemical wetting technique from organic metal salt solution. The subsequent step is transferring the deposited metallic substrate to chemical vapor deposition chamber and using ethene as carbon precursor to grow CNT at high temperature. The second step of preparation of sulfur-CNT composite is the incorporation of sulfur from sulfur-containing organic solvent toluene onto the vertically aligned CNT network. The aforementioned solvent evaporation method is used in this study to load massive amount of sulfur onto the vertically aligned CNT network. This innovatively synthesized CNT-sulfur composites perform multiple essential duties, such as effective suppression of soluble polysulfide dissolution, entrapment of extremely high loading mass of active material, provision of migration pathway for rapid ionic transportation, splendid mechanical stability, remarkable capacity of withstanding volume expansion during repeated charge-discharge cycles. The vertically aligned composite tremendously prolongs the life span of battery system and renders an excellent cycling stability. Some of the productive results are schematically illustrated in Figure 2-30 and Figure 2-31.

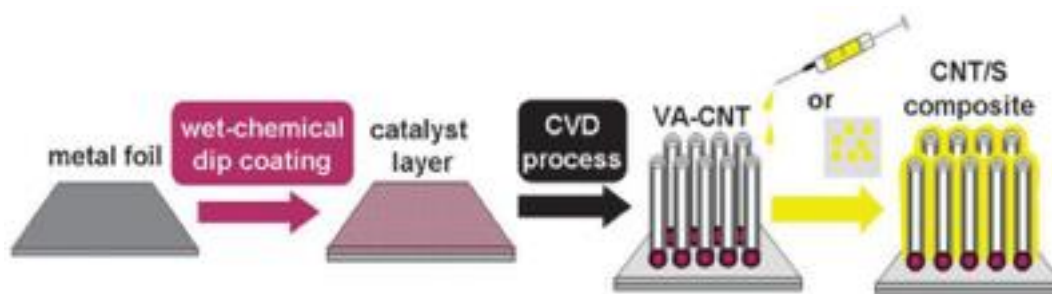


Figure 2- 30 Schematic of diagram of synthesis steps of cathode preparation [66].

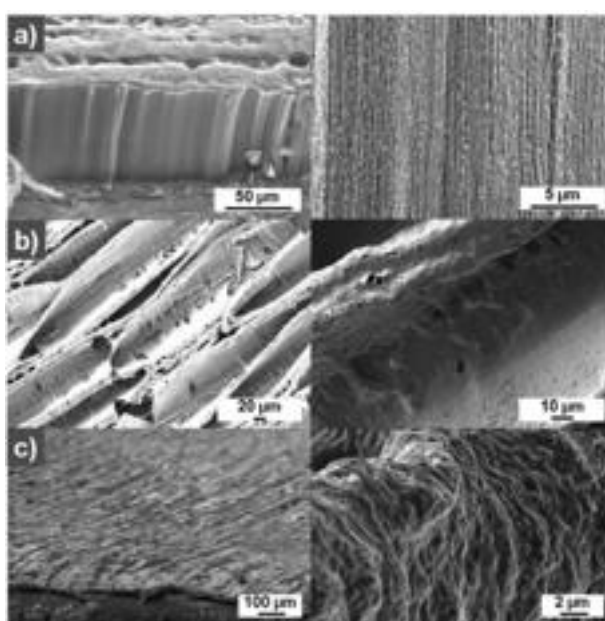


Figure 2- 31 SEM images of (a) CNTs (b) sulfur/VA-CNT composite (c) as-cycled sulfur/VA- CNT composite [66].

Yan et al. [67] reported that a rational and novel design of sulfurized carbon nanotubes composites is an appealing strategic method to accomplish long-life and high efficiency rechargeable lithium sulfur battery system. The innovative synthesis has received tremendous amount of attention from scientists all over the world due to its remarkable properties such as realization of one of the highest sulfur loading mass (as high as 68%) and significant decrease in weight along with tremendously simplified fabrication process owing to the absence of binder. Carbon nanotubes was selectively used as

sulfur carriers due to their hybridized  $sp^2$  carbon that leads to the formation of electrochemically active C-S bonds. Additionally, carbon nanotubes possess some other promising properties such as the ability to form oxygen-containing functional groups on the surface, superior mechanical strength and electrical conductivity. The sulfur can be firmly immobilized on the surface by those electrochemically active aromatic carbon rings through the formation of covalent bonds between oxygen atoms and sulfur atoms. In contrast to conventional preparation procedure of sulfur-CNT composite, the first step of preparation is dispersion of CNTs into a mixture of concentrated nitric acid and sulfuric acid to eliminate amorphous carbon and form oxygen- containing groups on the surface of CNTs. The subsequent procedure is the addition of hydrogen peroxide ( $H_2O_2$ ). The loading of sulfur onto the CNTs is achieved by aforementioned solvent evaporation method. Sulfur was dissolved into carbon disulfide ( $CS_2$ ) solution and then was added dropwise to form sulfur-CNTs composite. This innovatively synthesized CNT-sulfur composites perform multiple essential duties, such as effective suppression of soluble polysulfide dissolution, entrapment of extremely high loading mass of active material, provision of migration pathway for rapid ionic transportation, splendid mechanical stability, remarkable capacity of withstanding volume expansion during repeated charge-discharge cycles. The vertically aligned composite tremendously prolongs the life span of battery system and renders an excellent cycling stability. Some of the productive results are schematically illustrated in Figure 2-32 and Figure 2-33.

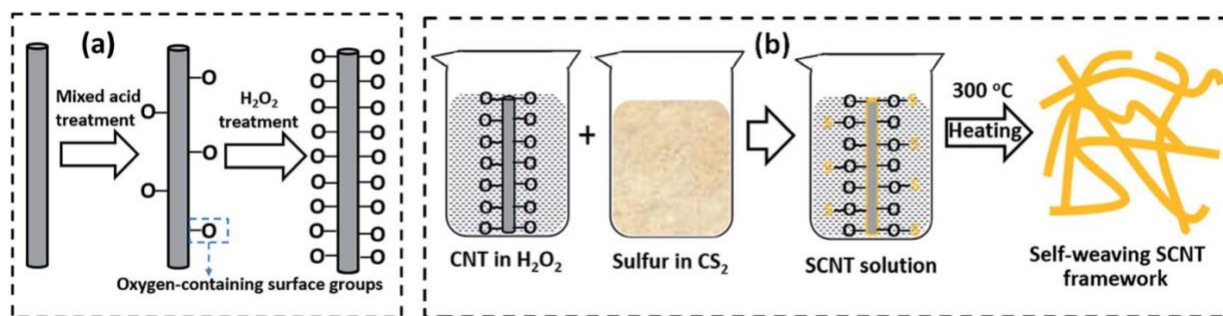


Figure 2- 32 Schematic diagram of synthesis steps of sulfur-CNTs [67].

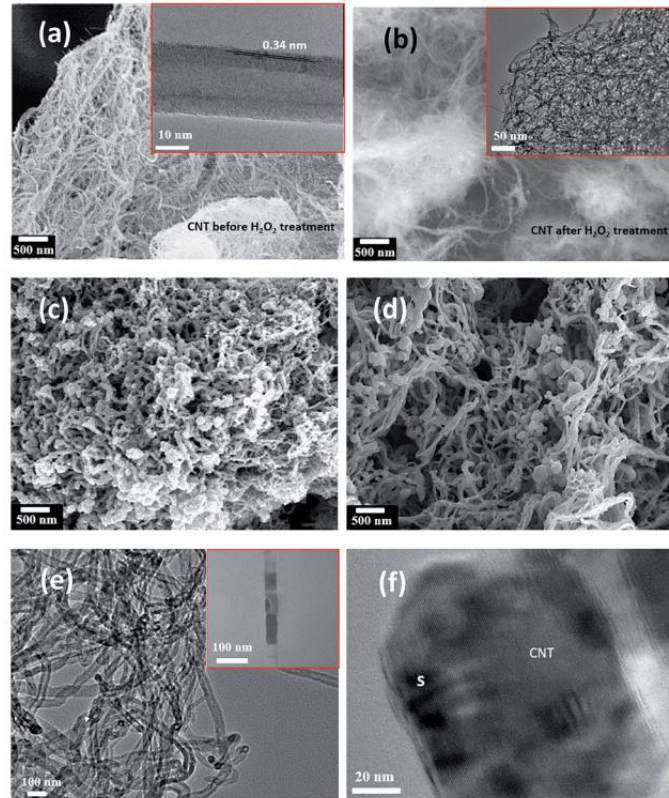


Figure 2- 33 Characterization of CNTs (a) before H<sub>2</sub>O<sub>2</sub> treatment and (b) after H<sub>2</sub>O<sub>2</sub> treatment (c) SCNT before heat treatment (d) SCNT after heat treatment (e) and (f) TEM image of SCNT after heat treatment [67].

### 2.3.2 Application of an interwoven self-supporting carbon nanotube layer

Su et al. [68] reported a facile and simple design of inserting a bi-functional, highly porous and self-supporting multi-walled carbon nanotube paper between the cathode and the separator is an appealing approach to alleviate the severe problems that lithium sulfur batteries face, aiming at large-scale production in the future. In contrast to traditional preparation procedure of sulfur-CNTs composite, the first step of preparation is dispersion of MWCNTs under ultrasonic condition. The subsequent step is a simple vacuum filtration without the presence of binders. The formation of large piece of MWCNT paper takes place and the formed MWCNT paper is collected by simply peeling off the filtration membrane. This innovatively synthesized MWCNT-sulfur composites perform multiple



essential duties, such as effective suppression of soluble polysulfide dissolution, entrapment of extremely high loading mass of active material, provision of migration pathway for rapid ionic transportation, splendid mechanical stability, remarkable capacity of withstanding volume expansion during repeated charge-discharge cycles. The composite tremendously prolongs the life span of battery system and renders an excellent cycling stability. Some of the productive results are schematically illustrated in Figure 2-34 and Figure 2-35.

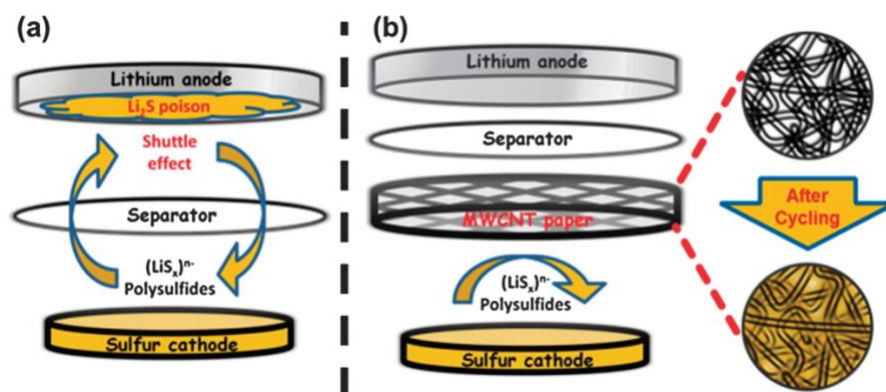


Figure 2- 34 Schematic diagram of the configuration of lithium sulfur battery (a) conventional configuration without the interlayer (b) novel configuration with WMCNT paper [68].

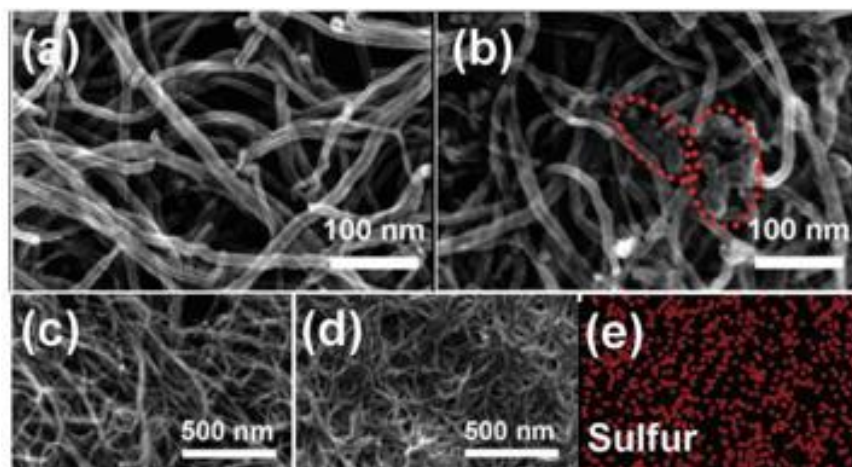


Figure 2- 35 Schematic diagram of morphology of MWCNT paper (a) before charge-discharge process (b) after 100 cycles (c) the morphology of raw tube before charge-discharge process (d) the structure of swollen tube after cycling (e) elemental mapping [68].



## **CHAPTER 3    POLYSULFIDE INFILTRATED FREE-STANDING CARBON CLOTH WITH CARBON BLACK COATING**

### **3.1 Overview**

To overcome the aforementioned challenges and issues of the LSBs, numerous novel and innovative approaches such as cathode modification, electrolyte optimization and protective layer on the surface of lithium metal anode have been developed as explained in the previous section. However, some of the techniques require complex synthesizing procedures hindering the mass production. In this work, a simple and effective cathode design is proposed to confine the sulfur preventing the shuttle effect and to increase the reaction sites to improve the utilization of the active materials, which leads to the enhanced capacity and the prolonged cycle lifetime of the LSBs. It uses a carbon cloth with carbon black coating to increase the surface area and provide the lithium polysulfide trapping sites. Lithium polysulfide is then infiltrated to achieve strong binding between the polysulfides and the carbon cloth. This chapter explains; 1) the material preparation procedure, 2) electrochemical tests to demonstrate the performance of the developed cathode, and 3) materials characterizations to confirm the effectiveness of the design.

### **3.2 Materials preparation**

#### **3.2.1 Preparation of carbon-black-coated carbon cloth**

A mixture of 90 wt% super P carbon black (SPCB) and 10 wt% PVDF was ground by a mortar and pestle for one hour and then dissolved into NMP to form a homogeneous slurry. The mixture was stirred overnight using magnetic stirrer. The carbon black coating was achieved by simply soaking the carbon cloth (cut to 14 mm diameter disc) into the previously obtained homogeneous slurry and letting it dry at ambient temperature overnight. This soaking and drying steps were repeated twice. The carbon-

black-coated carbon cloth is shown in Figure 3-1.

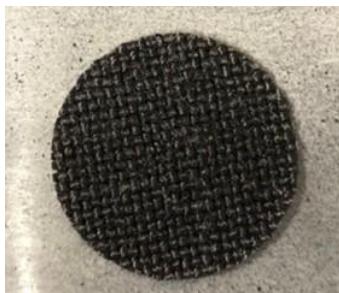


Figure 3- 1 Optical micrograph of carbon-black-coated carbon cloth

#### Preparation of $\text{Li}_2\text{S}_8$ -containing catholyte and infiltration of lithium polysulfide

First,  $\text{Li}_2\text{S}_8$ -containing catholyte was prepared following the procedure in ref [72]. 280 mg of sulfur and 58 mg of  $\text{Li}_2\text{S}$  were mixed in 4 ml of dimethoxyethane : dioxolane (DME:DOL, 1:1 v/v) solvent and stirred overnight at 60 °C. The  $\text{Li}_2\text{S}_8$ -containing catholyte is shown in Fig. 3-2. The dark brown solution had no residual solid particles indicating  $\text{Li}_2\text{S}$  and S was completely dissolved to form a  $\text{Li}_2\text{S}_8$  solution. Lithium polysulfide was implemented by simple drop casting the solution on the carbon-black-coated carbon cloth. The subsequent drying process was performed overnight inside a Ar-filled glovebox. Here, the solution was also drop-casted on a bare carbon cloth without carbon black coating as a reference.



Figure 3- 2 Schematic diagram of  $\text{Li}_2\text{S}_8$ -containing catholyte

### 3.2.2 Preparation of electrolyte

The electrolyte was prepared by dissolving 1M lithium bis(trifluoromethanesulfonyl) imide (LiTFSI) in DME:DOL (1:1 v/v). To promote the formation of a stable solid-electrolyte-interphase (SEI) on the surface of the metallic lithium anode during the repeated charge-discharge cycling process, 2 wt% of  $\text{LiNO}_3$  was added to the solution. These steps were conducted inside a Ar-filled glovebox.

### 3.2.3 Coin cell assembly

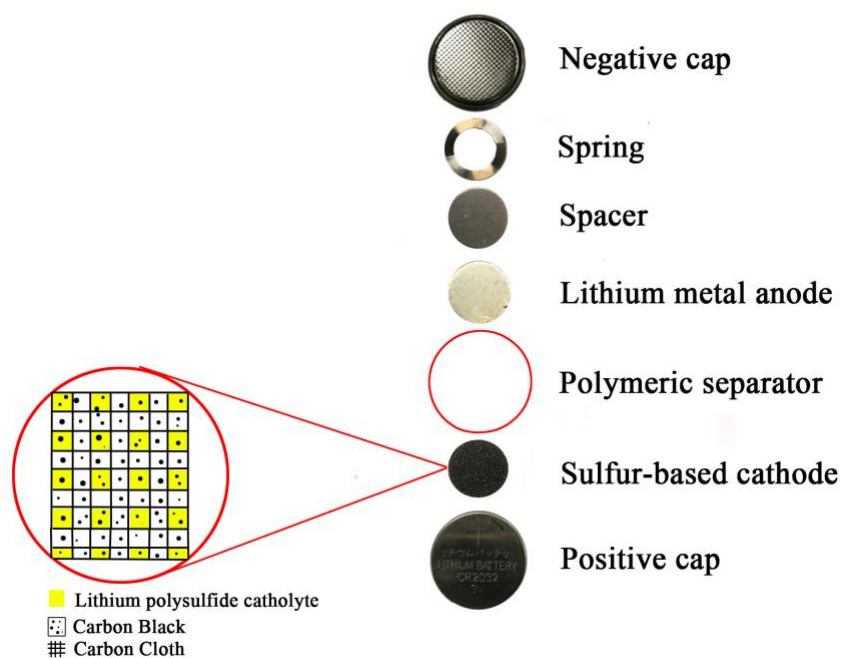


Figure 3- 3 Schematic diagram of coin cell assembly

Coin cells were assembled to test the electrochemical performance of the cathode. The sulfur-based cathode was obtained by simply applying the prepared catholyte on the commercial carbon cloth with a diameter of 14mm and the standard cell was assembled inside an Ar filled glovebox with oxygen level lower than 1 ppm by simply employing the key components of the battery cell such as sulfur-based cathode, lithium metal anode and electrolyte as schematically illustrated in Figure 3-3. To be specific,

lithium metal foil was polished by blade to remove the deposited oxide layer and expose the fresh lithium surface. And it was wetted with droplets of blank electrolyte (approximately 80  $\mu$ l). The subsequent step is placing a Celgard separator on top of the lithium metal foil. Subsequently, the self-supporting carbon cloth with carbon black coating with areal loading of approximately 2.47 mg/cm<sup>2</sup> was placed on top of the separator and The weight percentage of sulfur contained in the sulfur-based cathode was calculated by the equation shown below [73].

$$\text{Weight \% sulfur} = M_{sc}/(M_{sc} + M_{cc}),$$

where  $M_{sc}$  is mass of sulfur in the catholyte and  $M_{cc}$  is mass of carbon cloth with carbon black coating

The equivalent formula to calculate the sulfur loading wt% in a typical sulfur-carbon composite cathode is shown below [73]

$$\text{Weight \% sulfur} = M_{sc}/(M_{sc} + M_{cm} + M_{ca} + M_{pb} + M_{cc}),$$

Where  $M_{sc}$  is mass of sulfur in the cathode,  $M_{cm}$  is mass of carbon matrix,  $M_{ca}$  is mass of conductive additive,  $M_{pb}$  is mass of polymeric binder, and  $M_{cc}$  is mass of current collector

### 3.3 Sample morphology before cycling

Scanning electron microscopy (SEM) was used to analyze the structure of the carbon-black-coated carbon cloth.

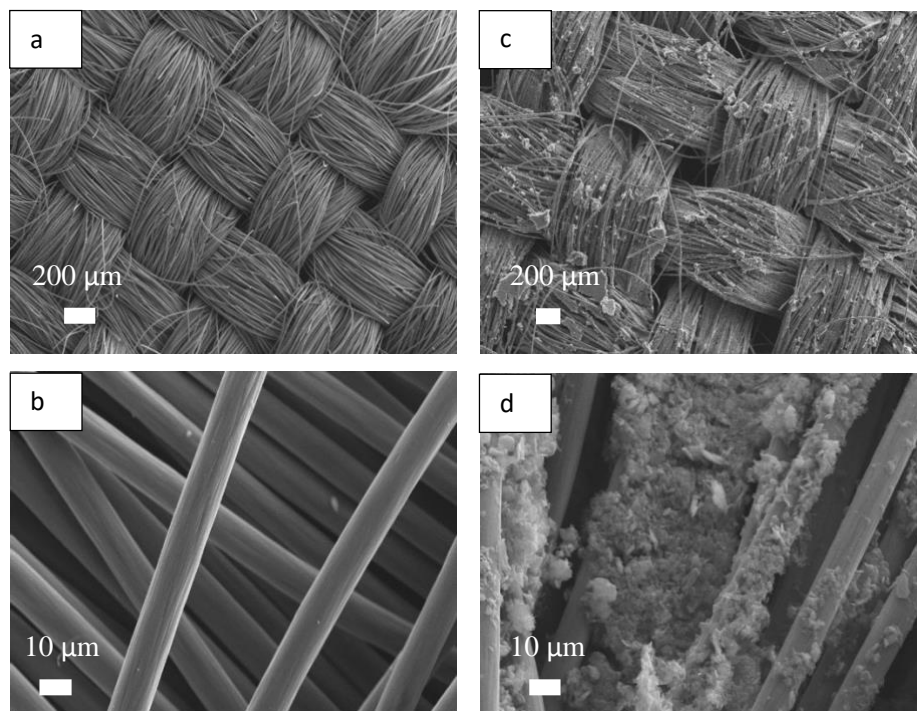


Figure 3- 4 (a-b) SEM images of interwoven self-supporting carbon cloth without carbon black coating. (c-d) SEM images of self-weaving carbon cloth with carbon black coating.

Figure 3-4 shows the morphological structure of the bare interwoven carbon cloth before and after electrically conductive carbon-black coating. Flat and smooth carbon fibers are clearly visible before the coating (a,b). The interwoven free-standing carbon cloth provides large internal voids, leading to high areal sulfur loading and enables conversion between long-chain polysulfide species to short-chain lithium sulfide to occur within a limited space. After the carbon-black coating, the presence of electrically conductive carbon black particles between the individual carbon nanofibers are clearly visible filling the empty spaces in the bare carbon cloth (c,d). An increase in reaction sites enabled by the electrically conductive carbon black coating is expected to realize strong bonding with polysulfide species.

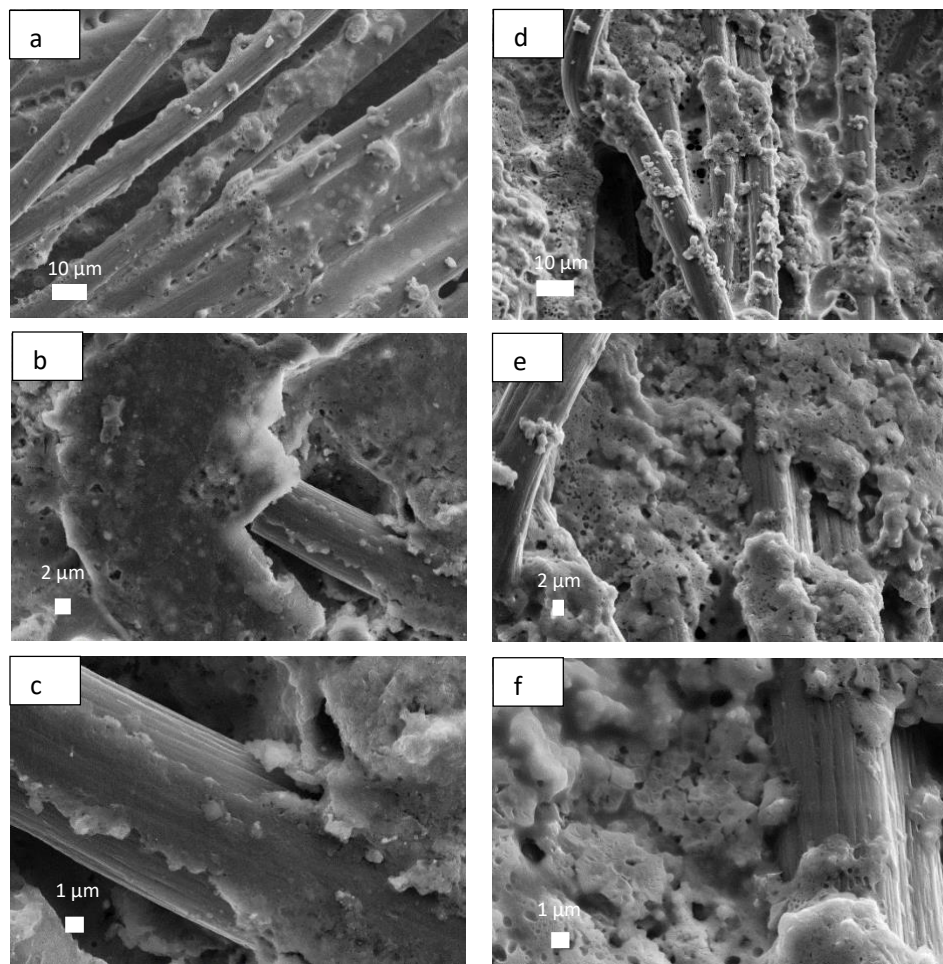


Figure 3- 5 Microstructural characterization of dissolved polysulfide electrode. (a-c) SEM images of sulfur-infiltrated carbon cloth without coating before cycling. (d-f) SEM images of sulfur-infiltrated carbon cloth with coating before cycling.

Figure 3-5 shows the morphology of  $\text{Li}_2\text{S}_8$ -infiltrated carbon cloth with and without carbon-black-coating. Large amounts of lithium polysulfide filled the void spaces between the carbon fibers in the bare carbon cloth (a-c). However, there remains empty spaces as there were large voids between the carbon fibers. On the other hand, the carbon cloth with carbon-black coating showed a uniform dispersion of the lithium polysulfide within a framework across the three- dimensional morphological skeleton of carbon cloth. This is because of the carbon-black particles filling the voids between the carbon fibers.

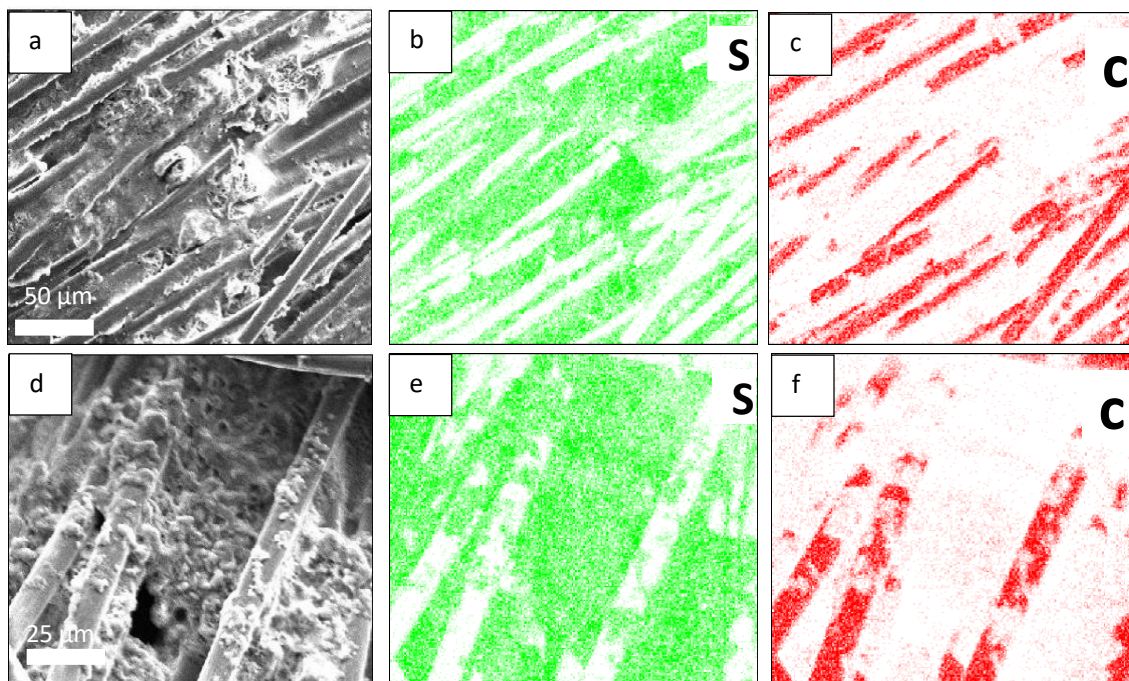


Figure 3- 6 (a-c) EDS data of sulfur-infiltrated carbon cloth without coating before cycling. (d-f) EDS data of sulfur-infiltrated carbon cloth with coating before cycling.

To confirm the sulfur dispersion within the carbon cloth, energy-dispersive X-ray spectroscopy (EDS) analysis was performed. Figure 3-6 shows the elemental mappings of S and C elements in the prepared catholyte samples. It clearly shows that sulfur is homogeneously distributed throughout both the coated and the uncoated carbon cloth samples. In the carbon-black coated sample, the carbon is also present in between the carbon clothes which implies a strong binding between sulfur and the carbon cloth. These results show the application of soluble polysulfide leads to a good dispersion of active material (sulfur) on the cathode, and strong entrapment of soluble polysulfide species is expected for the one with carbon black coating.



### 3.4 Electrochemical characterization

#### 3.4.1 Cyclic voltammetry (CV)

CV is a commonly used to study redox processes. This simple and facile method consists of a linear and a cyclic alteration of electrode potential between the working electrode and the reference electrode within a specific voltage window and the corresponding current flowing between the two electrodes is measured. CV involves repeated electrochemical cycles and the resultant current.

To test the electrochemical performance of the lithium-dissolved polysulfide cathode, CV analysis was performed for both bare carbon cloth without any coating and carbon cloth with carbon black coating. The scan rate for the cyclic voltammetry was set up at 0.1 mV/s between 1.0 and 3.0 V. The results are shown in Fig. 3-7. The two noticeable cathodic peaks are clearly visible. These peaks correspond to the conversion of elemental sulfur to soluble long-chain polysulfide species at 2.3 V and the subsequent transformation of soluble long-chain polysulfide to insoluble short-chain polysulfides ( $\text{Li}_2\text{S}$  and  $\text{Li}_2\text{S}_2$ ) at a lower voltage near 2.0 V. However, the carbon cloth with carbon black coating showed much higher current values compared to the one without coating. This drastic increase in the reaction current enhanced electrochemical reactivity. The increase in the reaction current was also observed for the anodic peaks indicating that the carbon black coating improved the delithiation process from  $\text{Li}_2\text{S}$  to S. The anodic peak for the carbon cloth without carbon black coating is located ~2.5 V with a shoulder at ~2.4 V. The peak shifted for the one with carbon black coating to 2.4 V and 2.3 V for the highest peak and the shoulder, respectively. This reduction in the polarization indicates that the reaction kinetics from  $\text{Li}_2\text{S}$  to S was improved by the carbon black coating corresponding to the increased surface area and the reaction sites.



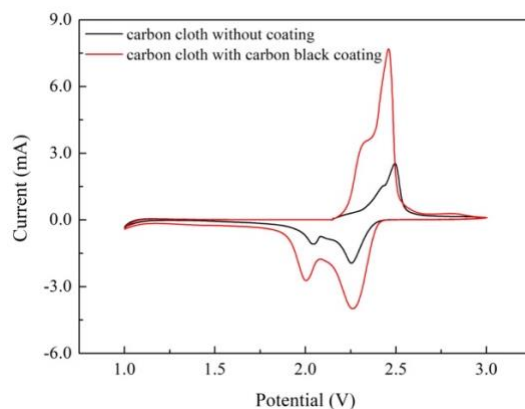


Figure 3- 7 Cyclic voltammograms of the Li/dissolved polysulfide batteries with uncoated carbon cloth and coated carbon cloth at a scan rate of 0.1 mV s<sup>-1</sup>.

### 3.4.2 Galvanostatic charge-discharge cycling

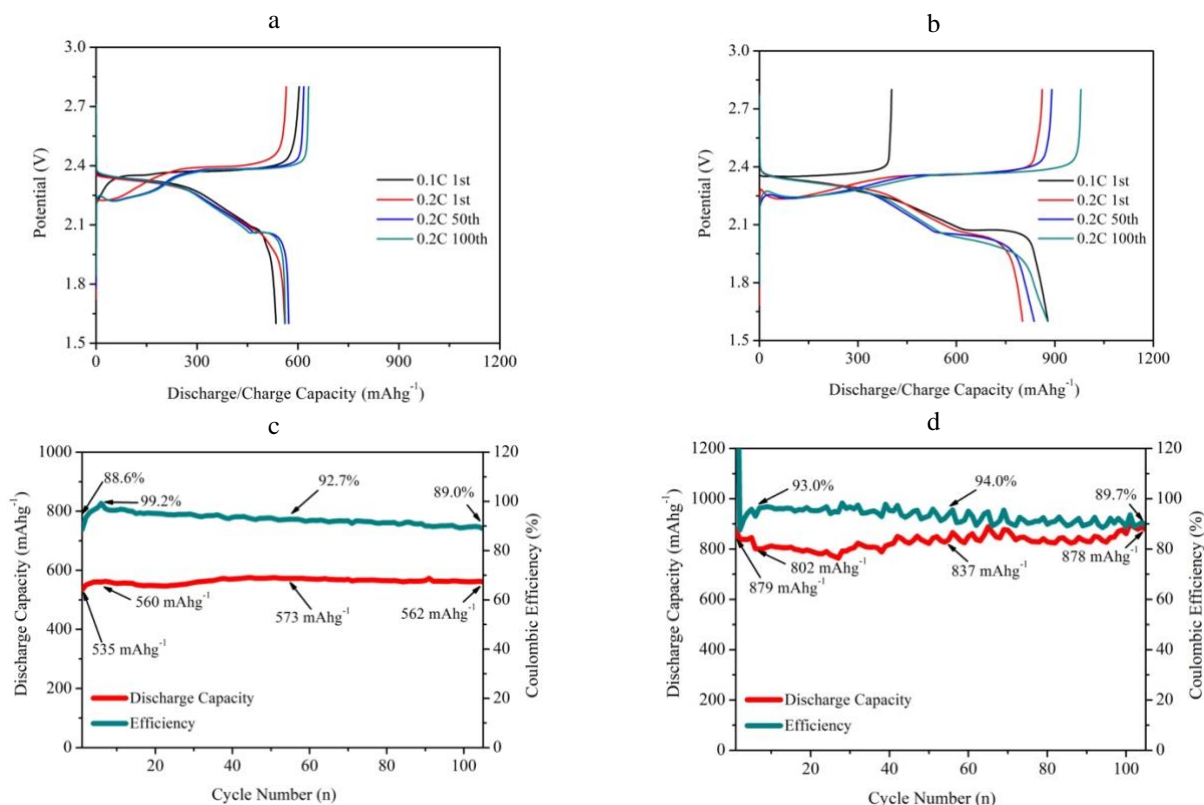


Figure 3- 8 a) Voltage vs discharge capacity and charge capacity profiles of the 1st at 0.1C, 1<sup>st</sup>, 50th , 100th at 0.2 C for uncoated carbon cloth. (b) Cyclability and Coulombic efficiency of the cell with uncoated carbon cloth. (c) Voltage vs discharge capacity and charge capacity profiles of the 1st at 0.1C, 1<sup>st</sup>, 50th , 100th at 0.2 C for coated carbon cloth. (d) Cyclability and Coulombic efficiency of the cell with coated carbon cloth.

The electrochemical performance of the cathode with and without carbon black coating was compared by galvanostatic charge-discharge cycle test. With charge and discharge cut off voltage set to 2.8 V and 1.6 V, respectively. For first cycle, 0.1 C was employed for the charge/discharge rate, and 0.2 C was used for the subsequent cycles. The results are shown in Figure 3-8. Two separate discharge plateaus in the discharge curves of coated sample are clearly visible, which correspond to the two cathodic peaks in the cyclic voltammetry curves (b). However, the second plateau is much shorter and for the one without coating (a). Carbon black coating played a pivotal role in the formation of the second flat stable plateau due to its strong bonding with polysulfide and numerous active reaction sites in the electrode composite. As a result, the carbon black coated cathode showed ~900 mAh/g capacity at the first cycle, while it was less than 600 mAh/g for the one without the coating. It is worth mentioning that the initial charge capacity for the carbon-black coated sample was approximately 400 mAh/g, which can be ascribed to the conversion from long-chain soluble  $\text{Li}_2\text{S}_8$  to elemental sulfur because  $\text{Li}_2\text{S}_8$ -containing catholyte was used as active material in this work, in contrast to the traditional sulfur loading approach. Those soluble polysulfide species rearranged themselves to suitable positions in the electrode during repeated charge-discharge cycling after the first cycle, leading to the high capacity in the following cycles as shown in Figure 3-8b. An increase in active reaction sites and strong bonding with soluble polysulfide species enabled by the electrically conductive carbon black coating realized successful entrapment of polysulfide and effectively utilized the active materials, leading to high capacity retention and flat stable voltage plateau. The cyclability and Coulombic efficiency of the uncoated sample and coated sample are shown in Figure 3-8 (c) and (d). This well-performed and cost-effective design provides coated Li/dissolved polysulfide batteries with superior capacity reversibility exceeding 780 mAh/g at current rate of 0.2 C over 100 cycles while it was less than 600 mAh/g for the one without coating. The coated sample retained approximately 100% of its initial capacity at the end of the 105th cycle, which is a strong indicator of significant reduction of soluble polysulfide dissolution

and diffusion through the electrolyte from the cathode to the anode.

### 3.4.3 Characterization of the samples after cycling

The coin-cells were disassembled after the battery cycle tests at the charged state and the electrodes were rinsed with the mixture of DME and DOL three times to remove the residual salt from the electrode. At the charged state the sulfur should be converted to  $\text{Li}_2\text{S}$  which is not soluble in the solvent mixture. The morphological changes of uncoated sample and coated sample were examined by SEM.

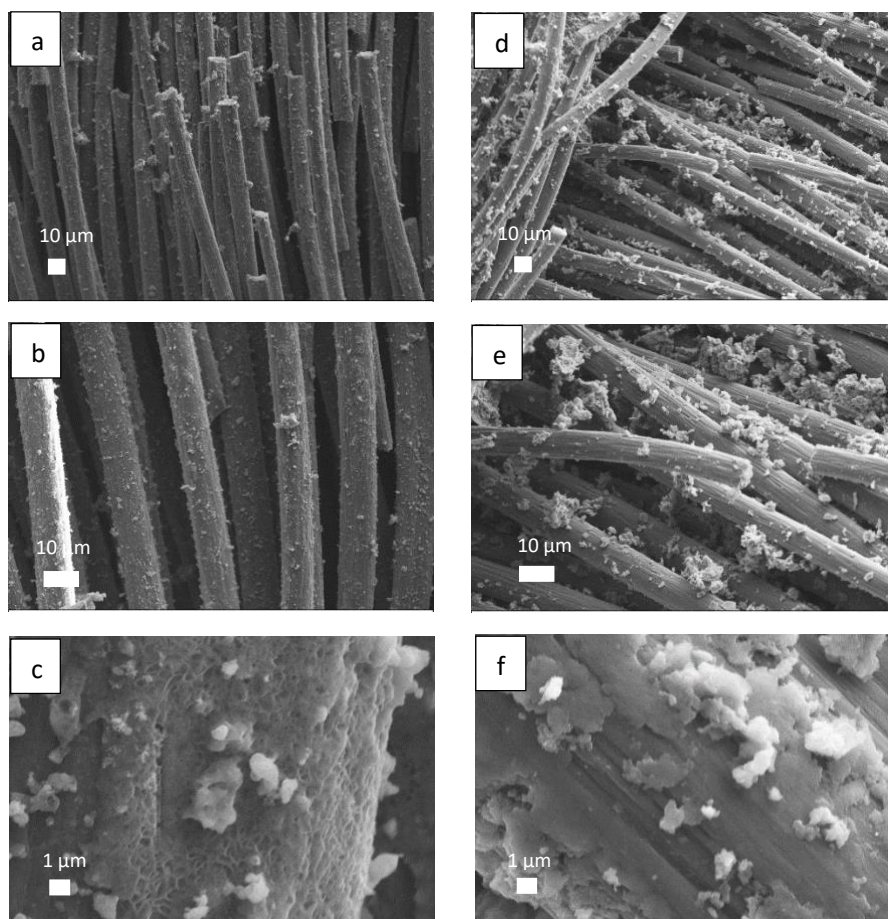


Figure 3- 9 (a-c) SEM images of  $\text{Li}_2\text{S}_8$ -infiltrated carbon cloth without coating after cycling. (d-f) SEM images of  $\text{Li}_2\text{S}_8$ -infiltrated carbon cloth with coating after cycling.

The morphology of the cycled cathode of uncoated sample and coated sample is shown in Figure

3-9. While only small number of particles is present on the bare carbon cloth without coating after 105 cycles, large amount of insoluble lithium sulfide on the surface of coated sample is observed. Almost all the catholyte films filling the void spaces in the bare carbon cloth before cycling disappeared. This confirms a successful inhibition of polysulfide diffusion for the carbon-black coated sample that contributed to its high capacity retention. At high magnification, the surface of the carbon fiber is covered by a porous film corresponding to the polysulfide dissolution (Fig. 3-9c). On the other hand, the carbon-black coated sample shows dense film on the surface (Fig. 3-9f). It is worth mentioning that the robust and cost-effective carbon cloth used as a current collector and as a host for active material simultaneously has a very uniform morphology after cycling, exhibiting the remarkable mechanical stability as schematically shown in high-magnification SEM images.

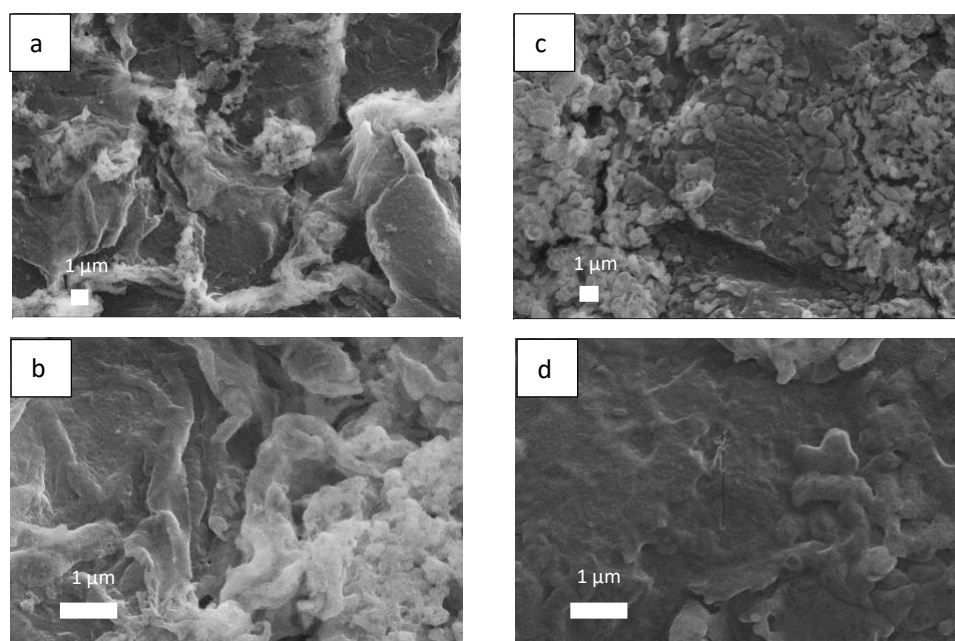


Figure 3- 10 (a-b) SEM images of cycled anode of uncoded sample after cycling. (c-d) SEM images of cycled anode of coated sample after cycling.

To further confirm the ability of the carbon black coating to suppress the polysulfide dissolution. The surface of the lithium anode was analyzed by SEM. Figure 3-10 compares the lithium anodes paired

with the cathode composite with and without carbon black coating. The surface of the lithium anode used in the cell with an uncoated sample showed cracks and uneven morphology. However, the surface of the lithium used with a carbon black coated sample is smooth particularly at the high magnification. The polysulfides reaching the anode surface was reduced to form  $\text{Li}_2\text{S}$  insulating the surface. This led to uneven deposition of lithium during charging. The smooth lithium deposition using carbon black coated sample indicates the lithium polysulfides were trapped in the cathode preventing the shuttle effect.

## CHAPTER 4 CONCLUSION

In summary, highly reversible Li/ dissolved polysulfide battery with self-weaving free- standing carbon cloth coated with electrically conductive carbon black was successfully prepared exhibiting excellent electrochemical performance in terms of capacity retention and inhibition of polysulfide diffusion. The interwoven, free-standing carbon cloth provides large internal voids. This results in a high areal sulfur loading ( $2.47 \text{ mg cm}^{-2}$ ) allowing conversion between long-chain polysulfide to short-chain lithium sulfide to occur within a limited space. Increased active reaction sites and strong bonding with soluble polysulfide species enabled by carbon black coating realizes highly effective utilization of active material, leading to high capacity retention and flat stable voltage plateau. This well-performed and cost-effective design provides coated Li/dissolved polysulfide battery with superior capacity reversibility exceeding  $780 \text{ mAh g}^{-1}$  and the Coulombic efficiency above 90% under current rate of 0.1C and 0.2C over 100 cycles compared to uncoated one.

## REFERENCES

- [1] Zhu, J., Zou, J., Cheng, H., Gu, Y., & Lu, Z. (2018). High energy batteries based on sulfur cathode. *Green Energy & Environment*. doi: 10.1016/j.gee.2018.07.001
- [2] Goodenough, J. (2015). Energy storage materials: A perspective. *Energy Storage Materials*, 1, 158-161. doi: 10.1016/j.ensm.2015.07.001.
- [3] Kang, W., Deng, N., Ju, J., Li, Q., Wu, D., & Ma, X. et al. (2016). A review of recent developments in rechargeable lithium–sulfur batteries. *Nanoscale*, 8(37), 16541-16588. doi: 10.1039/c6nr04923k.
- [4] Winter, M., Barnett, B., & Xu, K. (2018). Before Li Ion Batteries. *Chemical Reviews*, 118(23), 11433-11456. doi: 10.1021/acs.chemrev.8b00422
- [5] Wang, Y., Sahadeo, E., Rubloff, G., Lin, C., & Lee, S. (2018). High-capacity lithium sulfur battery and beyond: a review of metal anode protection layers and perspective of solid-state electrolytes. *Journal Of Materials Science*, 54(5), 3671-3693. doi: 10.1007/s10853-018-3093-7
- [6] Li, M., Lu, J., Chen, Z., & Amine, K. (2018). 30 Years of Lithium-Ion Batteries. *Advanced Materials*, 30(33), 1800561. doi: 10.1002/adma.201800561
- [7] Van Noorden, R. . (2014). The rechargeable revolution: a better battery. *Nature*, 507(7490), 26-28.

- [8] Bruce, P., Freunberger, S., Hardwick, L., & Tarascon, J. (2011). Li–O<sub>2</sub> and Li–S batteries with high energy storage. *Nature Materials*, 11(1), 19-29. doi: 10.1038/nmat3191
- [9] Nitta, N. , Wu, F. , Lee, J. T. , & Yushin, G. . (2014). Li ion battery materials: present and future. *Materials Today*, 18(5).
- [10] Yoshino, A. . (2012). The birth of the lithium-ion battery. *Angewandte Chemie International Edition*, 51(24), 0-0.
- [11] Tarascon, J. (2010). Key challenges in future Li-battery research. *Philosophical Transactions Of The Royal Society A: Mathematical, Physical And Engineering Sciences*, 368(1923), 3227-3241. doi: 10.1098/rsta.2010.0112
- [12] Bruce, P., Freunberger, S., Hardwick, L., & Tarascon, J. (2011). Li–O<sub>2</sub> and Li–S batteries with high energy storage. *Nature Materials*, 11(1), 19-29. doi: 10.1038/nmat3191
- [13] Lochala, J. , Liu, D. , Wu, B. , Robinson, C. , & Xiao, J. . (2017). Research progress towards the practical applications of lithium sulfur (li-s) batteries. *ACS Applied Materials & Interfaces*, acsami.7b06208.
- [14] Manthiram, A., Fu, Y., & Su, Y. (2012). Challenges and Prospects of Lithium–Sulfur Batteries. *Accounts Of Chemical Research*, 46(5), 1125-1134. doi: 10.1021/ar300179v
- [15] Barghamadi, M., Kapoor, A., & Wen, C. (2013). A Review on Li-S Batteries as a High Efficiency Rechargeable Lithium Battery. *Journal Of The Electrochemical Society*, 160(8),A1256-A1263. doi: 10.1149/2.096308jes



- [16] Fotouhi, A., Auger, D., O'Neill, L., Cleaver, T., & Walus, S. (2017). Lithium-Sulfur Battery Technology Readiness and Applications—A Review. *Energies*, 10(12), 1937. doi: 10.3390/en10121937
- [17] Whittingham, M.S., Lithium Batteries and Cathode Materials. *Chemical Reviews*, 2004.104(10): p.4271-4302
- [18] Manthiram, A. , Fu, Y. , Chung, S. H. , Zu, C. , & Su, Y. S. . (2014). Rechargeable lithium–sulfur batteries. *Chemical Reviews*, 114(23), 11751-11787.
- [19] Scheers, J., S. Fantini, and P. Johansson, A review of electrolytes for lithium–sulphur batteries. *Journal of Power Sources*, 2014. 255: p. 204-218
- [20] Xu, W., et al., Lithium metal anodes for rechargeable batteries. *Energy & Environmental Science*, 2014. 7(2): p. 513-537.
- [21] Wild, M., et al., Lithium sulfur batteries, a mechanistic review. *Energy & Environmental Science*, 2015. 8(12): p. 3477-3494.
- [22] Yu, X. , & Manthiram, A. . (2015). A class of polysulfide catholytes for lithium–sulfur batteries: energy density, cyclability, and voltage enhancement. *Phys. Chem. Chem. Phys.*, 17(3), 2127-2136.
- [23] Rauh, R. D.; Abraham, K. M.; Pearson, G. F.; Surprenant, J. K.; Brummer, S. B. A Lithium/Dissolved Sulfur Battery with an Organic Electrolyte. *Journal of The Electrochemical Society* 1979, 126, 523-527

- [24] Wu, M., J. Jin, and Z. Wen, Influence of a surface modified Li anode on the electrochemical performance of Li-S batteries. *RSC Advances*, 2016. 6(46): p. 40270- 40276
- [25] Wu, M., et al., Trimethylsilyl Chloride-Modified Li Anode for Enhanced Performance of Li–S Cells. *ACS Applied Materials & Interfaces*, 2016. 8(25): p. 16386-16395
- [26] Cheng, J.J., et al., Sulfur-Nickel Foam as Cathode Materials for Lithium-Sulfur Batteries. *ECS Electrochemistry Letters*, 2015. 4(2): p. A19-A21.
- [27] Xi, K., et al., Binder free three-dimensional sulphur/few-layer graphene foam cathode with enhanced high-rate capability for rechargeable lithium sulphur batteries. *Nanoscale*, 2014. 6(11): p. 5746-5753
- [28] Zhang, Y., et al., Three-dimensional carbon fiber as current collector for lithium/sulfur batteries. *Ionics*, 2014. 20(6): p. 803-808.
- [29] Gong, Z., et al., PEDOT-PSS coated sulfur/carbon composite on porous carbon papers for high sulfur loading lithium-sulfur batteries. *RSC Advances*, 2015. 5(117):p.96862-96869
- [30] Kong, L., Peng, H., Huang, J., & Zhang, Q. (2017). Review of nanostructured current collectors in lithium–sulfur batteries. *Nano Research*, 10(12), 4027-4054. doi: 10.1007/s12274- 017-1652-x.
- [31] Yuan, H., Huang, J., Peng, H., Titirici, M., Xiang, R., & Chen, R. et al. (2018). A Review of Functional Binders in Lithium-Sulfur Batteries. *Advanced Energy Materials*, 8(31), 1802107. doi: 10.1002/aenm.201802107.

- [32] Ya - Xia Yin, Xin, S. , Yu - Guo Guo, & Li - Jun Wan. (2013). Lithium–sulfur batteries: electrochemistry, materials, and prospects. *Angewandte Chemie International Edition*, 52.
- [33] Tan, J., Liu, D., Xu, X., & Mai, L. (2017). In situ/operando characterization techniques for rechargeable lithium–sulfur batteries: a review. *Nanoscale*, 9(48), 19001-19016. doi: 10.1039/c7nr06819k.
- [34] Barghamadi, M., Kapoor, A., & Wen, C. (2013). A Review on Li-S Batteries as a High Efficiency Rechargeable Lithium Battery. *Journal Of The Electrochemical Society*, 160(8), A1256-A1263. doi: 10.1149/2.096308jes.
- [35] Yamin, H. , & Peled, E. . (1983). Electrochemistry of a nonaqueous lithium/sulfur cell. *Journal of Power Sources*, 9(3), 281-287.
- [36] Yamaki, J. I. , Tobishima, S. I. , Sakurai, Y. , Saito, K. I. , & Hayashi, K. . (1998). Safety evaluation of rechargeable cells with lithium metal anodes and amorphous  $\text{V}_2\text{O}_5$  cathodes. *Journal of Applied Electrochemistry*, 28(2), 135-140.
- [37] Li, L. , Li, S. , & Lu, Y. . (2018). Suppression of dendritic lithium growth in lithium metal-based batteries. *Chemical Communications*, 54.
- [38] Tikekar, M. D. , Archer, L. A. , & Koch, D. L. . (2016). Stabilizing electrodeposition in elastic solid electrolytes containing immobilized anions. *Science Advances*, 2(7), e1600320-e1600320.
- [39] Orsini, F., Du Pasquier, A., Beaudoin, B., Tarascon, J., Trentin, M., & Langenhuizen, N. et al. (1998). In situ Scanning Electron Microscopy (SEM) observation of interfaces within plastic lithium batteries. *Journal Of Power Sources*, 76(1), 19-29. doi: 10.1016/s0378-7753(98)00128-

- [40] Liu, N. , Lu, Z. , Zhao, J. , Mcdowell, M. T. , Lee, H. W. , & Zhao, W. , et al. (2014). A pomegranate-inspired nanoscale design for large-volume-change lithium battery anodes. *Nature Nanotechnology*, 9(3), 187-192.
- [41] Qian, J. , Henderson, W. A. , Xu, W. , Bhattacharya, P. , Engelhard, M. , & Borodin, O. , et al. (2015). High rate and stable cycling of lithium metal anode. *Nature Communications*, 6, 6362.
- [42] Scheers, J. , Fantini, Sébastien, & Johansson, P. . (2014). A review of electrolytes for lithium–sulphur batteries. *Journal of Power Sources*, 255, 204-218.
- [43] Gao, J. , Lowe, M. A. , Kiya, Y. , & Abru?a, Héctor D. (2011). Effects of liquid electrolytes on the charge–discharge performance of rechargeable lithium/sulfur batteries: electrochemical and in-situ x-ray absorption spectroscopic studies. *The Journal of Physical Chemistry C*, 115(50), 25132-25137.
- [44] Mikhaylik, Y. V., Kovalev, I., Schock, R., Kumaresan, K., Xu, J., & Affinito, J. (2010). High energy rechargeable li-s cells for ev application: status, remaining problems and solutions.
- [45] Guo, J., & Liu, J. (2019). A binder-free electrode architecture design for lithium–sulfur batteries: a review. *Nanoscale Advances*, 1(6), 2104-2122. doi: 10.1039/c9na00040b

- [46] Yazami, R., & Touzain, P. (1983). A reversible graphite-lithium negative electrode for electrochemical generators. *Journal of Power Sources*, 9(3), 365-371.
  
- [47] Whittingham, M. S. . (1976). Electrical energy storage and intercalation chemistry. *Science*, 192(4244), 1126-1127.
  
- [48] Yin, Y., Xin, S., Guo, Y., & Wan, L. (2013). Lithium-Sulfur Batteries: Electrochemistry, Materials, and Prospects. *Angewandte Chemie International Edition*, 52(50), 13186-13200. doi: 10.1002/anie.201304762.
  
- [49] S.-E. Cheon, K.-S. Ko, J.-H. Cho, S.-W. Kim, E.-Y. Chin and H.-T. Kim, *J. Electrochem.Soc.*, 2003, 150, A796–A799.
  
- [50] Rehman, S. , Khan, K. , Zhao, Y. , & Hou, Y. . (2017). Nanostructured cathode materials for lithium–sulfur batteries: progress, challenges and perspectives. *J. Mater. Chem. A*, 5(7), 3014-3038.
  
- [51] D. Aurbach, E. Pollak, R. Elazari, G. Salitra, C. S. Kelley and J. Affinito, *J. Electrochem.Soc.*, 2009, 156, A694–A702.
  
- [52] Zhang, B., et al., Enhancement of long stability of sulfur cathode by encapsulating sulfur into micropores of carbon spheres. *Energy & Environmental Science*, 2010. 3(10): p. 1531-1537
  
- [53] Xin, S., et al., Smaller Sulfur Molecules Promise Better Lithium–Sulfur Batteries.*Journal of the American Chemical Society*, 2012. 134(45): p. 18510-18513

- [54] Ji, X., K.T. Lee, and L.F. Nazar, A highly ordered nanostructured carbon-sulphur cathode for lithium-sulphur batteries. *Nat Mater*, 2009. 8(6): p. 500-506.
- [55] Zheng, G., et al., Hollow Carbon Nanofiber-Encapsulated Sulfur Cathodes for High Specific Capacity Rechargeable Lithium Batteries. *Nano Letters*, 2011. 11(10): p. 4462-4467.
- [56] Zhang, C., et al., Confining Sulfur in Double-Shelled Hollow Carbon Spheres for Lithium–Sulfur Batteries. *Angewandte Chemie International Edition*, 2012. 51(38): p. 9592-9595.
- [57] Wang, D.-W., et al., A microporous-mesoporous carbon with graphitic structure for a high-rate stable sulfur cathode in carbonate solvent-based Li-S batteries. *Physical Chemistry Chemical Physics*, 2012. 14(24): p. 8703-8710.
- [58] Jayaprakash , N., et al., Porous Hollow Carbon@Sulfur Composites for High-Power Lithium–Sulfur Batteries. *Angewandte Chemie International Edition*, 2011. 50(26): p. 5904-5908.
- [59] Guo, J., Y. Xu, and C. Wang, Sulfur-Impregnated Disordered Carbon Nanotubes Cathode for Lithium–Sulfur Batteries. *Nano Letters*, 2011. 11(10): p. 4288-4294
- [60] Zhou, G., et al., A flexible nanostructured sulphur-carbon nanotube cathode with high rate performance for Li-S batteries. *Energy & Environmental Science*, 2012. 5(10): p.8901-8906.
- [61] Wei Seh, Z., et al., Sulphur-TiO<sub>2</sub> yolk-shell nanoarchitecture with internal void space for long-cycle lithium-sulphur batteries. *Nature communications*, 2013. 4: p. 1331-1331

- [62] Park, M.-S., et al., One-step synthesis of a sulfur-impregnated graphene cathode for lithium-sulfur batteries. *Physical Chemistry Chemical Physics*, 2012. 14(19): p. 6796- 6804.
- [63] Su, Y.-S., Y. Fu, and A. Manthiram, Self-weaving sulfur-carbon composite cathodes for high rate lithium-sulfur batteries. *Physical Chemistry Chemical Physics*, 2012.14(42): p. 14495-14499.
- [64] Wang, H., et al., Graphene-Wrapped Sulfur Particles as a Rechargeable Lithium– Sulfur Battery Cathode Material with High Capacity and Cycling Stability. *Nano Letters*, 2011. 11(7): p. 2644-2647.
- [65] Evers, S. and L.F. Nazar, Graphene-enveloped sulfur in a one pot reaction: a cathode with good coulombic efficiency and high practical sulfur content. *Chemical Communications*, 2012. 48(9): p. 1233-1235.
- [66] Dorfler, S., et al., High capacity vertical aligned carbon nanotube/sulfur composite cathodes for lithium-sulfur batteries. *Chemical Communications*, 2012. 48(34): p.4097-4099.
- [67] Yan, J., et al., Long-life, high-efficiency lithium/sulfur batteries from sulfurized carbon nanotube cathodes. *Journal of Materials Chemistry A*, 2015. 3(18): p. 10127- 10133.
- [68] Su, Y.-S. and A. Manthiram, A new approach to improve cycle performance of rechargeable lithium-sulfur batteries by inserting a free-standing MWCNT interlayer. *Chemical Communications*, 2012. 48(70): p. 8817-8819.
- [69] Inkson, B. (2016). Scanning electron microscopy (SEM) and transmission electron microscopy (TEM) for materials characterization. *Materials Characterization Using Nondestructive Evaluation (NDE) Methods*, 17-43. doi: 10.1016/b978-0-08-100040-3.00002-x

- [70] Huang, X., Wang, Z., Knibbe, R., Luo, B., Ahad, S., Sun, D., & Wang, L. (2019). Cyclic Voltammetry in Lithium–Sulfur Batteries—Challenges and Opportunities. *Energy Technology*. doi: 10.1002/ente.201801001.
- [71] Christopher D. Rahn and Chao-Yang Wang, “Battery System Engineering,” A John Wiley & Sons, Ltd., Publication (2013).
- [72] Yu, X., Zhou, G., & Cui, Y. (2018). Mitigation of Shuttle Effect in Li–S Battery Using a Self-Assembled Ultrathin Molybdenum Disulfide Interlayer. *ACS Applied Materials & Interfaces*, 11(3), 3080-3086. doi: 10.1021/acsami.8b19354.
- [73] Yu, X., Zhou, G., & Cui, Y. (2018). Mitigation of Shuttle Effect in Li–S Battery Using a Self-Assembled Ultrathin Molybdenum Disulfide Interlayer. *ACS Applied Materials & Interfaces*, 11(3), 3080-3086. doi: 10.1021/acsami.8b19354.